Neurog1 Can Partially Replace *Atoh1* to Differentiate and Maintain Hair Cells in a Disorganized Organ of Corti

Jahan I, Pan N, Kersigo J, Fritzsch B

Department of Biology, College of Liberal Arts & Sciences, University of Iowa, Iowa City, IA, USA

Key words: hair cells, survival, basic helix-loop-helix, transcription factors, development, misexpression, knockin

* Author for correspondence

Israt Jahan

University of Iowa, CLAS

Department of Biology

143, Biology Building

E-mail: israt-jahan@uiowa.edu

Phone: 319-335-1089

Bernd Fritzsch

University of Iowa, CLAS

Department of Biology

143, Biology Building

E-mail: bernd-fritzsch@uiowa.edu

Phone: 319353-2969

Funding: This work was supported by National Institute on Deafness and Other Communication Disorders (NIDCD) (R03 DC013655 to IJ) and Hearing Health Foundation (Emerging Research Grant to IJ). We thank the Office of the Vice President for Research (OVPR), University of Iowa College of Liberal Arts and Sciences (CLAS), and the P30 core grant for support (DC 010362). The funders had no role in study design, data collection and analysis, decision to publish, or preparation of the manuscript.

Abstract:

Atoh1, a basic helix-loop-helix transcription factor (TF), is essential for the differentiation of hair cells (HCs), mechanotransducers that convert sound into auditory signals in the mammalian organ of Corti (OC). Previous work demonstrated that replacing mouse *Atoh1* with the fly ortholog *atonal* rescues HC differentiation, indicating functional replacement by other bHLH genes. However, replacing *Atoh1* with *Neurog1* resulted in reduced HC differentiation compared to transient *Atoh1* expression in a 'self-terminating' *Atoh1* conditional null mouse (*Atoh1-Cre; Atoh1*$^{f/f}$). We now show that combining *Neurog1* in one allele with removal of floxed *Atoh1* in a 'self-terminating' conditional mutant (*Atoh1-Cre; Atoh1*$^{f/kiNeurog1}$) mouse results in significantly more differentiated inner HCs and outer HCs that have a prolonged longevity of nine months compared to *Atoh1* 'self-terminating' littermates. Stereocilia bundles are partially disorganized, disoriented and not HC type specific. Replacement of *Atoh1* with *Neurog1* maintains limited expression of *Pou4f3* and *Barhl1* and rescues HCs quantitatively, but not qualitatively. OC patterning as well as supporting cell differentiation is also partially disrupted. Diffusible factors involved in patterning are reduced (*Fgf8)* and factors involved in cell interactions are changed (*Jag1, Hes5).* Despite presence of many HCs with stereocilia these mice are deaf, possibly related to HC and OC patterning defects. This study provides a novel approach to disrupt OC development through modulating the HC specific intracellular TF network. The resulting disorganized OC indicates that normally differentiated HCs act as 'self-organizers' for OC development and that *Atoh1* plays a critical role to initiate HC stereocilia differentiation independent of HC viability.

Introduction:

Neurosensory development requires sequential, coordinated activation and cross-regulation of numerous transcription factors (TFs) to define precursors and initiate differentiation of the various cell types of the nervous and sensory system (Fritzsch et al., 2015; Imayoshi and Kageyama, 2014; Reiprich and Wegner, 2014). Molecularly dissecting these interactions requires model systems with limited cellular diversity and stereotyped cellular patterning. The organ of Corti (OC) is such a model system with hair cells (HCs) and supporting cells (SCs) organized into the most stereotyped cell assembly of vertebrates (Slepecky, 1996) suited to detect minute aberrations (Jahan et al., 2013). The stereotyped cellular pattern may allow the molecular dissection of the intricate interaction of multiple basic helix-loop-helix (bHLH) proteins (Benito-Gonzalez and Doetzlhofer, 2014; Fritzsch et al., 2010b) to define HCs/SCs.

Targeted deletion studies in mice have demonstrated that three bHLH TFs (*Neurog1, Neurod1, Atoh1*) are essential to differentiate neurons and HCs of the inner ear (Bermingham et al., 1999; Fritzsch et al., 2006; Fritzsch et al., 2010b). These loss-of-function analyses also revealed cross-regulation among these bHLH TFs. For example, *Neurog1* null mice showed loss of HCs (Ma et al., 2000; Matei et al., 2005), apparently through alteration of *Atoh1* expression (Raft et al., 2007). While absence of *Neurog1* reduced HCs, absence of *Neurod1* resulted in ectopic HCs in ganglia (Jahan et al., 2013). Changes in *Atoh1* expression may be mediated through cross-regulation of *Neurod1* downstream of *Neurog1* (Jahan et al., 2010). *Neurod1*, in turn, may suppress *Atoh1* in the ear (Jahan et al., 2013), comparable to the cerebellum (Pan et al., 2009).

Other loss-of-function studies showed that *Atoh1* drives HC differentiation (Bermingham et al., 1999; Fritzsch et al., 2005; Pan et al., 2011) and overexpression of *Atoh1* transformed non-sensory cells into HCs (Kelly et al., 2012; Zheng and Gao, 2000). *Atoh1* differentiates HCs in the ear and level and duration of *Atoh1* expression regulates different types of HCs and their viability (Jahan et al., 2013; Sheykholeslami et al., 2013). Consistent with these data, 'self-terminating' *Atoh1* (*Atoh1-Cre; Atoh1*$^{f/f}$) mouse initiated near normal HC differentiation but rapidly lost most HCs by 3 weeks (Pan et al., 2012a), a loss also reported in inducible cre lines (Cai et al., 2013; Chonko et al., 2013). Replacing both alleles of *Atoh1* with another bHLH TF, *Neurog1* (*Atoh1*$^{kiNeurog1/kiNeurog1}$) resulted in very few immature HCs bearing microvilli with a central kinocilium (Jahan et al., 2012). This inability

of *Neurog1* to maintain and differentiate HCs below even transient *Atoh1* expression (Pan et al., 2012a) contrasts with work on retinal ganglion cells (RGCs) in which the *Atoh1* paralog, *Atoh7*, was replaced by *Neurod1* (Mao et al., 2008). *Neurod1* can replace *Atoh7*, possibly because RGC precursors are pre-programmed to differentiate as RGCs independent of the type of bHLH TF (Mao et al., 2013). The pairing of *Atoh1/Neurog1* is molecularly as different as the *Atoh7/Neurod1* pairing (52% sequence similarity versus 60%), suggesting that overall binding differences may not fully explain these very different results in eyes and ears. We reasoned that failure of functional replacement of *Atoh1* by *Neurog1* in the ear (Jahan et al., 2012), compared to *Atoh7* by *Neurod1* in the retina (Mao et al., 2008), or *Atoh1* by the fly *atonal* (Wang et al., 2002), could either relate to 'self-regulation' of *Atoh1* via its enhancer (Helms et al., 2000) or to a unique functional requirement of Atoh1/atonal protein to initiate HC differentiation.

To test these possibilities, we generated a new mouse model (*Atoh1-Cre; Atoh1*$^{f/kiNeurog1}$) with insertion of *Neurog1* in one allele of *Atoh1* (Jahan et al., 2012) and removal of the second floxed *Atoh1* allele by 'self-terminating' with *Atoh1-Cre* (Pan et al., 2012a). This novel composite mouse mutant can differentiate most HC and can rescue many HC for up to nine months. However, HCs stereocilia are variably disorganized, OC patterning is disrupted, and mice are deaf despite near normal numbers of rather well differentiated HCs.

Results:

Neurog1 expression in HCs with transient expression of Atoh1

We previously demonstrated that *Neurog1* replacement in both alleles of *Atoh1* resulted in expression of *Neurog1* in HC precursors that differentiate multiple microvilli (Jahan et al., 2012). Like *Atoh1* null mutant mice (Bermingham et al., 1999), homozygous *Neurog1* knockin mice die after birth, precluding postnatal analysis. *Atoh1* auto-regulates its own expression by activating *Atoh1* specific enhancer (Helms et al., 2000). We speculated that replacement of *Atoh1* by *Neurog1* in both alleles might have failed to activate the enhancer for adequate *Neurog1* expression under *Atoh1* promoter control (Jahan et al., 2012). To overcome this problem, we generated a novel mouse model that combined *Neurog1* knockin in one *Atoh1* allele with a floxed second *Atoh1* allele, the latter to be excised by *Atoh1-Cre* (*Atoh1-Cre; Atoh1*$^{f/kiNeurog1}$; Figure 1a). This newly developed *Atoh1-Cre; Atoh1*$^{f/kiNeurog1}$ model resulted in viable mice, overcoming the neonatal lethality of homozygous *Neurog1* knockin mice (Jahan et al., 2012). *Atoh1*$^{f/+}$ or *Atoh1*$^{f/f}$ mice without *Atoh1-Cre* were used as a 'control' in this study except for the RT-qPCR analysis where *Atoh1*$^{+/kiNeurog1}$ mice was used as control to compare *Neurog1* expression in the *Atoh1-Cre; Atoh1*$^{f/kiNeurog1}$ mice.

In situ hybridization (ISH) showed that *Neurog1* knockin into the *Atoh1* locus (*Atoh1-Cre; Atoh1*$^{f/kiNeurog1}$) resulted in expression of *Neurog1* in OC HCs not detected in control littermates (Figure 1b, b'). At P0, the *Atoh1-Cre; Atoh1*$^{f/kiNeurog1}$ mutant showed very little *Atoh1* expression in the apex (Figure 1c, c'). In contrast, a downstream target of *Atoh1*, *Pou4f3,* was strongly expressed in the HCs of P0 *Atoh1-Cre; Atoh1*$^{f/kiNeurog1}$ OC (Figure 1d, d') whereas expression of *Barhl1* was delayed compared to the vestibular epithelia at P0 (Figure 1e,e'). At P7, qPCR showed relative mRNA expression for *Neurog1*, *Pou4f3* and *Barhl1* in *Atoh1-Cre; Atoh1*$^{f/kiNeurog1}$ cochlea that was reduced compared to the *Atoh1*$^{+/kiNeurog1}$ cochlea, but the reduction was not statistically significant (*Atoh1*$^{+/kiNeurog1}$ expression was normalized to 1, Figure 1f). In 'self-terminating' *Atoh1-Cre; Atoh1*$^{f/f}$ mice, both *Pou4f3* and *Barhl1* showed patchy loss at P0 (Pan et al., 2012a). In contrast, *Neurog1* misexpression revealed expression of both *Pou4f3* and *Barhl1* until P7 (Figure 1f). Partial expression of *Pou4f3* and *Barhl1* might improve HC viability as HCs are rapidly lost in either *Pou4f3* (Hertzano et al., 2004; Xiang et al., 2003) or *Barhl1* null mutants (Li et al., 2002).

Neurog1 misexpression with transient expression of Atoh1 results in HC maintenance

Immunohistochemistry of Myo7a (a hair cell specific marker) at P7 revealed formation of an almost continuous row of IHCs and two-three rows of OHCs in the *Neurog1* misexpressing mice (Figure 2). There were occasionally two rows of IHCs. Extra rows of IHCs coincide with absence of inner pillar (IP) cells, shown by immunohistochemistry of acetylated Tubulin (highly expressed in SCs), next to the extra row of IHCs (Figure 2b-c"'). There was no indication that the length of the cochlea was changed (Table S1). The third row of OHCs disappeared toward the base of the cochlea, including formation of some gaps in OHCs (Figure 2c-d"'). Tubulin immunohistochemistry labeled differentiated IP, outer pillar (OP) cells and many Deiters' cells at P7 (Figure 2). Overall, *Neurog1* misexpression resulted in considerable increase in HC and SC formation compared to the *Atoh1-Cre; Atoh1$^{f/f}$* mice that had mostly one row of OHCs and only few IHCs at P7 (Figure 3). We conclude that *Neurog1* misexpression combined with transient *Atoh1* expression can partially substitute for *Atoh1* to differentiate and maintain HCs compared to the massive loss of nearly all HCs in 'self-terminating' mice (Pan et al., 2012a). Diminished long-term viability of HCs correlates with reduced TFs known to be essential for HC viability (*Pou4f3, Barhl1*).

More HCs form in Atoh1-Cre; Atoh1$^{f/kiNeurog1}$ than Atoh1-Cre; Atoh1$^{f/f}$ mice

We next quantified the Myo7a positive HCs, identifying IHCs as being medial and OHCs lateral to Tubulin immunopositive IP/OP cells. We counted all cells in a 300 µm length near the apex (10%), near the middle (50%) and near the base of the cochlea (90%) in comparable segments from control, *Atoh1-Cre; Atoh1$^{f/kiNeurog1}$* and *Atoh1-Cre; Atoh1$^{f/f}$* littermates (Figure 3d,e; Table S2; N=6). The numbers of IHCs were significantly higher in the *Atoh1-Cre; Atoh1$^{f/kiNeurog1}$* mice than the *Atoh1-Cre; Atoh1$^{f/f}$ mice* ($p< 0.01$; Figure 3d). The IHC counts between *Atoh1-Cre; Atoh1$^{f/kiNeurog1}$* mice and control littermate showed no significant difference (Figure 3d). In summary, replacement of one allele of *Atoh1* by *Neurog1* combined with a 'self-terminating' second *Atoh1* allele rescued most IHCs compared to the massive loss of IHCs in the *Atoh1-Cre; Atoh1$^{f/f}$* mouse.

The quantification of OHCs demonstrated that significantly more OHCs form in the *Atoh1-Cre; Atoh1$^{f/kiNeurog1}$* mice compared to *Atoh1-Cre; Atoh1$^{f/f}$* mice (Figure 3e; $p< 0.01$). In contrast to IHCs, OHCs in *Atoh1-Cre; Atoh1$^{f/kiNeurog1}$* mice were significantly reduced

compared to the OHCs in control littermate (Figure 3b, $p < 0.05$). *Neurog1* increased survival preferentially of IHCs with the greatest reduction in the third row of OHCs (Figure 2c-d"', 3b, 3e). Previous work on 'self-terminating' *Atoh1* conditional null mice (Pan et al., 2012a) and *Atoh1* hypomorphs (Sheykholeslami et al., 2013) showed a differential loss of OHCs with the third row being most susceptible whereas tamoxifen induced *Atoh1-Cre* wiped out all HCs rapidly (Cai et al., 2013; Chonko et al., 2013).

HCs survive longer in Atoh1-Cre; Atoh1$^{f/kiNeurog1}$ mice than Atoh1-Cre; Atoh1$^{f/f}$ mice

We next investigated the longevity of these HCs using Myo7a and Tubulin immunohistochemistry (Figure 4). At nine months, many Myo7a positive HCs remained in the *Atoh1-Cre; Atoh1$^{f/kiNeurog1}$* mice. In particular, many IHCs survived medial to Tubulin positive IP cells but OHCs showed patchy loss (Figure 4b-b"). This contrasted with severe HC loss in the *Atoh1-Cre; Atoh1$^{f/f}$* mice where only few HCs survived to nine months (Figure 4c-c"), essentially being lost by 3 weeks (Pan et al., 2012a). In addition to HCs, SCs also persisted longer in the *Atoh1-Cre; Atoh1$^{f/kiNeurog1}$* mice and many more Tubulin positive pillar cells and Deiter's cells were observed compared to *Atoh1-Cre; Atoh1$^{f/f}$* mice (Figure 4b', b", c', c").

Atoh1-Cre; Atoh1$^{f/kiNeurog1}$ mice are deaf, despite presence of most HCs

Proper arrangement of cells is essential for the function of the OC to enable sound perception (Cai et al., 2003; Jacobo and Hudspeth, 2014). To assess the hearing function in *Neurog1* misexpressing mice, we measured at P30 Auditory Brainstem Response (ABR) to click stimuli (Figure 5). ABRs showed no auditory response in the *Atoh1-Cre; Atoh1$^{f/kiNeurog1}$* mice compared to control littermates (Figure 5). We concluded that expression of *Neurog1* developed and maintained many HCs in a non-functional OC. We next investigated possible reasons for this functional defect, focusing first on stereocilia of hair cells.

Replacing Atoh1 by Neurog1 results in aberrant stereocilia bundle formation.

HC function critically depends on the normal development of the stereocilia bundles that mediate mechanotransduction (Hudspeth, 2014; Jacobo and Hudspeth, 2014; Sienknecht et al., 2014). Loss, alteration or reduction of *Atoh1* results in abnormal stereocilia bundle formation (Chonko et al., 2013; Pan et al., 2012a), if any bundle forms at all (Pan et al., 2011). *Atoh1* dosage and timing of expression is important for the proper stereocilia

development and maturation (Jahan et al., 2013). Several mutations that interfere with stereocilia bundle organization and homeostasis are known (Hertzano et al., 2008; Kitajiri et al., 2010; Mogensen et al., 2007; Sekerková et al., 2011) and many of these mutations result not only in aberrant bundle morphology but in death of hair cells (Kersigo and Fritzsch, 2015b; Self et al., 1998; Ueyama et al., 2014). Consistent with a role of *Atoh1* in stereocilia differentiation is that forced expression of *Atoh1* can restore hair bundles (Yang et al., 2012). To go beyond the obvious increase in HC survival (Figure 2-4) and to better understand the apparent deafness (Figure 5), we next investigated how replacement of *Atoh1* with *Neurog1* influenced stereocilia formation and thus function of HCs. We examined at least three cochlea of the *Atoh1-Cre; Atoh1*$^{f/kiNeurog1}$ mutant and the littermate controls each at three different stages (P1, P7 and P22) with scanning electron microscopy (SEM; Figures. 6-7). We found that onset of the stereocilia bundle differentiation in *Neurog1* misexpressing mice was delayed (Figure 6a-b"). The bundles were immature with formation of similar length of microvilli surrounding a central kinocilium at P1 (Figure 6b-b"). Control littermates displayed already the staircase pattern of progressively increasing length of stereocilia modiolar to an acentric kinocilium (Figure 6a). This stunted stereocilia growth was more obvious in OHCs than IHCs, especially in the second and third rows of OHCs of *Atoh1-Cre; Atoh1*$^{f/kiNeurog1}$ mice. At P7, the bundles formed nearly normal staircase pattern in the apex of the cochlea in the *Atoh1-Cre; Atoh1*$^{f/kiNeurog1}$ mice whereas the basal HCs displayed aberrations such as fusion or loss of stereocilia, predominantly in the third row of OHCs (Figure 6 c-d").

SEM revealed progressive deformations of the stereocilia bundles in *Atoh1-Cre; Atoh1*$^{f/kiNeurog1}$ mice (Figure 7). The stereocilia bundle of IP cells were neither indicative of IHCs or OHCs. Some HCs in the *Neurog1* misexpressing mice had stereocilia bundles without staircase organization, some stereocilia were fused with each other or showed stunted growth (marked with cyan arrows in Figure 7). SEM also revealed that the thickness of the stereocilia of some IHCs in the *Atoh1-Cre; Atoh1*$^{f/kiNeurog1}$ mice was altered to look like OHCs, indicating partial cell fate switching of some IHCs to OHCs (marked with the red arrows in Figure 7). Beyond the fusion and ectopic stereocilia formation, the SEM in the *Neurog1* misexpressing mice also revealed disruption of the boundaries between adjacent HCs (Figure 7). Some HCs touched each other without intervening SCs in *Atoh1-Cre; Atoh1*$^{f/kiNeurog1}$ mice (marked with green arrows in Figure 7). In P7 and P22 mice, we found ectopic stereocilia bundles protruding from the apical surfaces of the IP cells (marked with

yellow arrows, Figure 7). This altered pattern of HCs and SCs indicated disruptions of cell-cell interactions. We therefore further analyzed the molecular basis of OC pattern formation (Fritzsch et al., 2014b; Groves and Fekete, 2012) focusing on genes known to affect OC development.

We previously demonstrated conversion of OHCs into IHCs in *Neurod1* conditional deletion mice (Jahan et al., 2010). Absence of *Neurod1* resulted in premature and altered *Atoh1* and *Fgf8* expression and transformation of thin OHC stereocilia into thick IHC stereocilia (Jahan et al., 2010, 2013). Essentially, *Atoh1* and *Fgf8* expression was not suppressed by *Neurod1* (Jahan et al., 2010). Therefore, we investigated the expression of *Neurod1* and *Fgf8* in the *Atoh1-Cre; Atoh1*$^{f/kiNeurog1}$ mice as opposite effect (conversion of stereocilia of IHC to OHC) was observed in the *Neurog1* misexpressing mice. Misexpression of *Neurog1* resulted in stronger and earlier expression of *Neurod1* in the E16.5 *Atoh1-Cre; Atoh1*$^{f/kiNeurog1}$ cochlea compared to control littermates (Figure 8a-b"). *Fgf8* expression was patchy and much reduced in some IHCs of the E16.5 *Atoh1-Cre; Atoh1*$^{f/kiNeurog1}$ mice (Figure 8d', Figure S1b'). The alteration of HC stereocilia diameter in *Atoh1-Cre; Atoh1*$^{f/kiNeurog1}$ mice might relate to the locally altered level of *Atoh1*/*Neurog1* signaling that distorted the specificity of HC types. How *Atoh1* signal level alteration mechanistically regulates the thickness of the stereocilia bundles, possibly through modulation of whirlin (Mogensen et al., 2007), requires further work.

Among microRNAs, specifically, *miR-96* was reported for proper maturation and organization of the stereocilia bundle (Kuhn et al., 2011; Lewis et al., 2009). Single base mutation in the *miR-96* gene resulted in non-syndromic, progressive hearing loss in human (Kuhn et al., 2011; Lewis et al., 2009). *miR-96* is expressed in the sensory epithelia of the mouse cochlea (Weston et al., 2011a). We previously reported very limited *miR-96* expression only in the apex of the *Atoh1*$^{kiNeurog1/kiNeurog1}$ cochlea (Jahan et al., 2012) or near absence in conditional *Atoh1* null mice (Pan et al., 2011). Both mutants showed no HC differentiation beyond precursors cells. In the *Atoh1-Cre; Atoh1*$^{f/kiNeurog1}$ mice, *miR-96* expression was almost normal except for the basal hook region where it showed some gaps (Figure 8e-f'). How possible alterations of some of the miR's tie into stereocila development through repression of relevant genes remains speculative.

Neurog1 misexpression alters OC patterning and SC differentiation.

Given the formation of stereocilia bundles on IP cells (Figure 7), we investigated next the distribution of an IP cell specific marker, *Ngfr (p75)* (von Bartheld et al., 1991). ISH of *p75* confirmed the selective expression of *p75* in the IP cells in the P0 control mice (Figure 9a). In P0 *Atoh1-Cre; Atoh1*$^{f/kiNeurog1}$ mice, *p75* expression was patchy near the base (Figure 9b'-b") but continuous in the apical half of the cochlea (Figure 9b). Consistent with stereocilia bundles on IP cells (Figure 7a-c), immunohistochemistry for HC specific Myo7a subsequent to *p75* ISH showed that the gaps in the *p75* positive IP cells were filled with the Myo7a positive HCs (Figure 9b"). We also performed dual immunohistochemistry using p75 and Myo7a antibodies with different fluorophore labelling of the secondary antibodies. Double immunohistochemistry also showed that the gaps of p75 immunopositive IP cells were filled with Myo7a positive putative HCs (Figure 9c-d"). Combined with stereocilia formation in the apical surfaces of the IP cells in the *Atoh1-Cre; Atoh1*$^{f/kiNeurog1}$ mice, our data suggested that expression of *Neurog1* transformed some IP cells into a hybrid of IP and HCs.

To further assess this possibility, we quantified the Tubulin immunopositive IP cells in P7 *Atoh1-Cre; Atoh1*$^{f/kiNeurog1}$ mice (Figure 9e). There was a reduction of Tubulin positive IP cells in the *Neurog1* misexpressing mice relative to control littermates in the apex ($p< 0.05$) and middle ($p<0.01$) turn of the cochlea. Despite this presumed transformation, overall IP cell formation was increased in *Atoh1-Cre; Atoh1*$^{f/kiNeurog1}$ relative to *Atoh1-Cre; Atoh1*$^{f/f}$ mice ($p< 0.01$). While p75 is an excellent marker for IP cells, differentiation of IP cells remains normal in *p75* null mice and its function remains obscure (Tan et al., 2010).

Pillar cell formation was abnormal in *Fgf8* null mice (Jacques et al., 2007; Mueller et al., 2002). As previously reported (Jacques et al., 2007; Pirvola et al., 2000), *Fgf8* is expressed in all IHCs. In the *Atoh1-Cre; Atoh1*$^{f/kiNeurog1}$ mice, downregulation of *Fgf8* expression might affect the diffusible signal strength from IHCs to nearby SCs (Groves and Fekete, 2012). Given the defects in IP cells, we next double labeled *Fgf8* and *p75* ISH and revealed the reduction of *Fgf8* expression was correlated with the reduction of *p75* positivity in the *Atoh1-Cre; Atoh1*$^{f/kiNeurog1}$ mice (Figure S1a-c'). Previous work also demonstrated that *Atoh1* is transiently expressed in the IP cells (Driver et al., 2013; Matei et al., 2005). Signals that prevent IP cells to differentiate as HCs might be disrupted in the *Atoh1-Cre;*

Atoh1$^{f/kiNeurog1}$ mice, resulting in partial transdifferentiation of some IP cells into HCs (Figure 7).

We also investigated the *Fgf10* and *Bmp4* that flanked the medial and lateral borders of the OC, respectively (Figure S1d,d'). In the P0 *Atoh1-Cre; Atoh1*$^{f/kiNeurog1}$ mice, *Fgf10* was drastically reduced and *Bmp4* showed expanded expression toward OC making gaps where OC cells were replaced by simple epithelium (Figure S1d,d').

To obtain further molecular insights into the SC differentiation, we studied *Prox1* expression by ISH in the *Neurog1* misexpressing mice (Fritzsch et al., 2010a). *Prox1* was expressed in almost all the SCs, except for some reduction in the IP cells in P0 *Atoh1-Cre; Atoh1*$^{f/KiNeurog1}$ mice (Figure 10a-b"). These data suggested that several reliable markers of SC differentiation were altered, lost or even replaced by HC markers, indicating that expression of *Neurog1* in HCs affected other cells of the OC.

Neurog1 expression alters Notch ligand and Notch effector gene expression.

Atoh1 expression in HCs regulates the expression of genes in the Delta/Notch signaling pathway for the development of the surrounding SCs and maintains the proper patterning of the OC (Kobayashi and Kageyama, 2014; Sprinzak et al., 2011; Yamamoto et al., 2014). Lack of Notch ligand, *Jag1* results in extra rows of IHCs and loss of OHCs (Brooker et al., 2006; Kiernan et al., 2006). Downstream target genes of Notch, the Hes/Hey factors play important roles for the proper specification of the SCs by negatively regulating pro-neuronal bHLH TFs (Doetzlhofer et al., 2009; Zine and de Ribaupierre, 2002). Given the lack of proper patterning of HCs/SCs in the OC, we investigated the expression of *Jag1* and *Hes5* by ISH in the *Atoh1-Cre; Atoh1*$^{f/KiNeurog1}$ mice (Figure 10). In the P0 control mice, *Jag1* was widely expressed in the GER and in the SCs, particularly in the IP cells (Figure 10c-c'). In the *Atoh1-Cre; Atoh1*$^{f/kiNeurog1}$ mice, the expression of *Jag1* was slightly reduced in both GER and the SCs with some patchy loss toward the base (Figure 10d-d').

At E14.5 *Hes5* was found in the mid-base of the control cochlea (Figure S2a). E14.5 *Atoh1-Cre; Atoh1*$^{f/kiNeurog1}$ mice had delayed *Hes5* expression (Figure S2d). *Hes5* was upregulated at later stages (Figure S2e,f), showed patchy expression in the GER and in the SCs in *Atoh1-Cre; Atoh1*$^{f/kiNeurog1}$ mice (Figure 10e-f', S2e,f). We combined *Hes5* ISH with Myo7a immunohistochemistry to detect if the downregulation of *Hes5* was associated with

HCs differentiation in the *Neurog1* expressing mice (Figure S2g-h") as previously reported after *Hes5* loss (Zine and de Ribaupierre, 2002). Myo7a positive HCs showed no correlation with the patchy loss of *Hes5* expression in this mutant (Figure S2g-h").

Alteration of *Jag1* and *Hes5* expression in *Atoh1-Cre; Atoh1*$^{f/KiNeurog1}$ mice indicated the potential effects of *Neurog1* on the expression of these genes, and thus with the Delta/Notch signaling. These altered HC-SC communication might disrupt the OC patterning (Figure 7), but did not result in overproduction of HCs (Figure S2h-h") as in *Hes/Hey* mutants. (Benito-Gonzalez and Doetzlhofer, 2014; Zine et al., 2001). How changes in intracellular HC gene expression through replacement of *Atoh1* by *Neurog1* alter intercellular signaling and disrupt the mosaic of the OC, remains unclear.

In conclusion, near normal numbers of HC can be generated by combining transient *Atoh1* expression with *Neurog1* misexpression, but these HCs have variably defected stereocilia bundles and organization of OC. Despite long-term viable HCs, the abnormal OC organization obfuscates hearing. OC disorganization may be a consequence of expression changes of *Fgf8* that may form secondary signaling centers comparable to the midbrain hindbrain boundary (Fritzsch et al., 2014a; Lee et al., 1997) but also due to altered cellular interactions (Groves and Fekete, 2012).

Discussion:

A fundamental information of neurosensory development needed for regeneration is understanding the molecular basis for the generation of topologically distinct cell fates out of uniform progenitor populations (Fritzsch et al., 2014a; Imayoshi and Kageyama, 2014; Reiprich and Wegner, 2014). Precise spatial and temporal control of gene expression by different combinations of TFs establish the molecular code to determine the cell fate (Guillemot, 2007). Molecular dissection of this complexity requires models of limited cellular diversity in a stereotyped arrangement to evaluate minute deviations from normal, for example in the ommatidia of flies (Johnston and Desplan, 2014). The OC of the mammalian inner ear is another excellent model organ with stereotyped cellular patterning that allows the exploration of molecularly induced deviations of developmental processes mediated by intra- and extracellular patterning processes (Fritzsch et al., 2014b; Groves and Fekete, 2012). Our data suggest a profound effect of the intracellular signals via cell-cell interactions and altered diffusible factors on the cellular and organ patterning process.

Neurog1 cooperates with transient Atoh1 expression to develop and maintain HCs.

One approach of probing signal specificity of a given TF in developing gene regulation networks is replacing them by closely related TFs (Guillemot, 2007). Replacing *Atoh7* with *Neurod1* leads to normal differentiation of RGCs whereas replacing *Neurod1* by *Atoh7* alters the cell fate of amacrine and photoreceptors cells into RGCs (Mao et al., 2013; Mao et al., 2008) indicating context dependency of gene actions. We knocked *Neurog1* into the *Atoh1* locus to test whether a bHLH TF that is in the ear and the brain exclusively associated with proliferative precursors (Imayoshi and Kageyama, 2014; Ma et al., 2000) can function in differentiation to maintain or alter HC precursor differentiation. We previously showed that *Atoh1*$^{kiNeurog1/kiNeurog1}$ can effectively drive *Neurod1* in HC precursors (Jahan et al., 2012) but can neither initiate normal HC development nor maintain viability of HC precursors. We also showed that 'self-terminating' *Atoh1* results in very limited viability of HCs with incomplete stereocilia differentiation (Pan et al., 2012a). Our quantitative assessment of the HCs formation in *Atoh1-Cre; Atoh1*$^{f/kiNeurog1}$ mice of this study indicates that *Neurog1* misexpression partially rescues HC loss and maintains HCs for a longer period, compared to 'self-terminating' *Atoh1* conditional null mice (Pan et al., 2012a). *Neurog1* cannot maintain the basal third row of OHCs that depend on *Fgf20* released from SCs (Huh et al., 2012), a factor which may be affected in our mice due to alteration in SC development.

Our data suggest that HC precursors behave like RGCs (Mao et al., 2008) and show limited flexibility to respond to the distantly related bHLH TF *Neurog1* with anything but enhanced HC differentiation relative to that of transient *Atoh1* expression. This diverges from spiral ganglion neurons that differentiate readily as HCs if suppression of *Atoh1* is removed by eliminating *Neurod1* (Jahan et al., 2010). *Atoh1* is required for an unknown initial step of HC differentiation neither *Neurog1* nor *Neurod1* can replace and thus no HCs differentiate in homozygotic *Atoh1*$^{kiNeurog1/kiNeurog1}$ mice (Jahan et al., 2012). Obviously, the fly *atonal* gene can replace *Atoh1* (Wang et al., 2002) and HCs can partially differentiate in the reduced (Sheykholeslami et al., 2013) or transient expression of *Atoh1* (Pan et al., 2012a), or even in the absence of *Atoh1* in chimeric mice (Du et al., 2007). Elucidating the molecular basis of this critical step of downstream gene activation (Cai et al., 2015; Pan et al., 2012b) for which *Atoh1* expression cannot be substituted by *Neurog1* could help to transform stem cells more effectively into HCs (Ronaghi et al., 2014; Zine et al., 2014).

Atoh1 cooperates with unknown factors to fully express *Pou4f3* (Ahmed et al., 2012) which, in turn, cooperates with *Atoh1* to maintain HCs (Chen et al., 2015; Hertzano et al., 2004; Masuda et al., 2012; Xiang et al., 2003). In contrast to *Pou4f3*, *Barhl1* expression depends exclusively on *Atoh1* (Chellappa et al., 2008). *Barhl1* is required for HC survival even in presence of *Atoh1* and *Pou4f3* (Li et al., 2002). *Atoh1-Cre; Atoh1*$^{f/KiNeurog1}$ mice have near normal expression of *Pou4f3*, but show delay and progressive reduction of *Barhl1* (Fig. 1). We suggest that *Neurog1* may activate a second pathway for near normal *Pou4f3* expression (Ahmed et al., 2012; Masuda et al., 2012), but fails to fully activate *Barhl1* needed for HC maintenance (Figure 11). Our mouse model is useful to test the ability of putative regulators of downstream genes to enhance HC viability through the regulation of *Pou4f3* and *Barhl1* expression.

Replacement of Atoh1 by Neurog1 alters stereocilia differentiation.

Closer investigation of the cochlea of the *Neurog1* misexpressing mice revealed various irregularities in stereocilia bundles and their distribution in the OC (Figure 6-7):

1. Irregular length of individual stereocilia within the bundles.
2. Uncoupling of stereocilia diameter from HC type.
3. Appearance of ectopic stereocilia bundles on IP cells.
4. Stereocilia bundles being abnormally fused with each other.

Stereocilia are necessary for hearing (Müller and Barr-Gillespie, 2015). Despite the rescue of overall HC formation, *Atoh1-Cre; Atoh1*$^{f/kiNeurog1}$ mice show no ABR and are deaf (Figure 5). Whether this was due to HCs or the disorganization of the OC requires future single cell recordings on isolated HCs. We presume that the irregularities in stereocilia bundles, the essential features of mechanoelectric transduction (Hudspeth, 2014), preclude normal function of many HCs. Loss of *Pou4f3*, but not of *Barhl1* causes stereocilia bundle aberrations (Chellappa et al., 2008; Hertzano et al., 2004). Reduced level of *Pou4f3* transcripts at or after P7 may contribute to the bundle aberration that develops mostly in late postnatal stages in *Neurog1* misexpressing mice (Figure 7). Actin is a major protein of stereocilia (Müller and Barr-Gillespie, 2015) and stereocilia homeostasis is essential for HC function and viability (Kersigo and Fritzsch, 2015a; Self et al., 1999; Ueyama et al., 2014). Deregulation of actin bundling has been associated with HC dysfunction and loss (Mogensen et al., 2007; Perrin et al., 2010; Rzadzinska et al., 2009; Taylor et al., 2015). Various myosins, actins and a rich variety of actin bundling proteins are regulated downstream of Atoh1 to transform microvilli into stereocilia during development (Kitajiri et al., 2010; Schwander et al., 2010). Loss of microRNA (miR) is also associated with derailed stereocilia development (Weston et al., 2011b). *Neurog1* misexpression results in near normal *miR-96* expression but other miR's could be altered that also affect stereocilia formation. Once causality between Atoh1 and downstream signals associated with various bundle aberrations is clearer, our mouse model could help to eliminate spurious relationships as it has partially uncoupled stereocilia differentiation from HC topology.

Replacement of Atoh1 by Neurog1 alters the patterning of the OC.

The OC is highly stereotyped in its organization with two distinctly patterned compartments separated by a single row of adjacent IP cells, which express *Atoh1* (Driver et al., 2013; Fritzsch et al., 2014b; Matei et al., 2005) without differentiating into HCs. Expression of multiple Hes/Hey factors (Benito-Gonzalez and Doetzlhofer, 2014; Doetzlhofer et al., 2009; Petrovic et al., 2014) may block these cells from HC development. Notch inhibition (and thus reduced expression of *Hes/Hey*) may lead to HC differentiation of IP cells (Mizutari et al., 2013). *Neurog1* misexpression affects IP cells in multiple ways, including formation of HC-like stereocilia bundles and replacement by the HC marker Myo7a in *p75* positive IP cell. These instabilities in IP cells may relate to the alteration in Notch signaling as observed (Figure 9, 10).

In addition, the disruption of OC patterning is in part due to alterations in the Delta/Notch signaling pathway. For example, *Jag1* and downstream target gene *Hes5* are altered. Previous work on *Jag1* loss showed reduction in total number of HCs (Kiernan et al., 2006). *Neurog1* misexpression results in discontinuity of *Jag1* and delayed upregulation and differential downregulation of *Hes5* in the cochlea. These expression changes vary radially and longitudinally, providing additional modulations of the variable signals of diffusible factors such as *Fgf8, Fgf10 or Bmp4.* Combined with altered SC response properties through changes in *p75* and *Prox1*, these local changes may relate to the random OC patterning defects.

In summary, we demonstrate that misexpression of *Neurog1* provides partial functional replacement of *Atoh1* in in developing HC and improves HC maintenance. *Neurog1* misexpression changes the signaling pattern of diffusible factors originating from HCs, as well as cell-cell interactions via Delta/Notch; both alterations contribute to the disorganization of the OC. Previous reports on deletion of different combinations of *Hes1*, *Hes5* or *Hey2* show changes in sensory patterning in support of the lateral inhibition model, but mutants mostly maintain the HC and SC mosaic formation (Doetzlhofer et al., 2009; Zine et al., 2001). Changes of proneural bHLH genes in HCs alters the overall patterning of the OC presumably by altering intercellular interactions via diffusible factors (*Fgf8*) and cell-cell interactions. Understanding the causalities of these alterations and translating such understanding into regeneration (Zine et al., 2014) could help to restore hearing in deaf patients, the fastest growing ailment of seniors worldwide (Kersigo and Fritzsch, 2015b;

Müller and Barr-Gillespie, 2015). Beyond addition or deletion of entire rows of HCs obtained with past mutations (Doetzlhofer et al., 2009; Zine et al., 2001), we provide here a new model of a dysfunctional OC that can help in OC restoration attempts. Rendering through additional manipulation the dysfunctional OC of our new mouse model into a functional one able to hear could provide proof of principle for various fledgling attempts to achieve the goal of transforming a partially defunct elderly OC into a fully functional OC.

Material and Methods:

Ethics guidelines

All animal procedures were carried out according to the recommendations and guidelines of the University of Iowa Institutional Animal Care and Use Committee (IACUC) for use of laboratory animals in this research and the protocol was approved (ACURF # 1309175).

Combining *Neurog1* knockin (*Atoh1*^{kiNeurog1}) with 'self-terminating' *Atoh1* mice (*Atoh1-Cre; Atoh1*$^{f/kiNeurog1}$)

Construction of *Neurog1* knockin plasmid and generation of the *Atoh1*^{kiNeurog1} mouse model was previously described (Jahan et al., 2012). To generate the *Atoh1-Cre; Atoh1*$^{f/kiNeurog1}$ line, we bred the heterozygous *Neurog1* knockin mice (*Atoh1*$^{+/kiNeurog1}$) (Jahan et al., 2012) with mice carrying *Atoh1-Cre* transgene with one *Atoh1* floxed allele (*Atoh1-Cre; Atoh1*$^{f/+}$) as described previously (Pan et al., 2012a).

Genotyping

Mice were genotyped using tail DNA for standard PCR amplification as described previously (Jahan et al., 2012; Pan et al., 2012a). For further details, see the supplementary Materials and Methods.

In situ hybridization

In situ hybridization was performed as previously described (Jahan et al., 2012) using the RNA probe labeled with digoxigenin. Detailed description is in supplementary Materials and Methods.

RT-qPCR

For quantitative reverse transcription and polymerase chain reaction (RT-qPCR), we used the P7 cochlea from the *Atoh1-Cre; Atoh1*$^{f/kiNeurog1}$ mice and their littermate heterozygous *Atoh1*$^{+/kiNeurog1}$ as control. After sedation with 2,2,2 tribromoethanol, the mice were hemisected and the cochleae were dissected out within 2-3 minutes in RNase free condition and stored in RNAlater in -80°C. Total RNA extraction was performed using the Direct-zol RNA Mini-Prep kit from Zymo research and RNA concentration and 260/280 ratio was obtained in Nanodrop spectrophotometer. On-column DNase-I treatment was performed according to the Direct-zol Kit protocol. 1 µg of total RNA was reverse transcribed and cDNA was synthesized with Anchored-oligo $(dT)_{18}$ primer using the Transcriptor First Strand cDNA Synthesis Kit from Roche. For qPCR, the primers and probes were designed from Roche Universal Probe Library Assay design center (http://lifescience.roche.com/shop/CategoryDisplay?catalogId=10001&tab=&identifier=Universal+Probe+Library&langId=-1) and primers were obtained from the Integrated DNA Technologies. The primers sequences and the priming conditions are listed in the Table S3. qPCR was performed in ninety-six well plate using Roche's Light Cycler 480 Probes Master in a Roche 480 Light Cycler real-time PCR machine. For all target genes, qPCR was performed in at least 3-4 biological replicates and 3 technical replicates including no template controls for each sample following MIQE guidelines (Bustin et al., 2009). q-PCR data was analyzed in Microsoft Excel and delta delta C_T was calculated using the Livak method to determine the relative expression in the *Atoh1-Cre; Atoh1*$^{f/kiNeurog1}$ cochlea compared to control normalized to Actb reference transcript. Statistical analysis was performed using student's t-test in the GraphPad Prism 6 software.

Immunohistochemistry and Cell Counts

Immunohistochemistry was performed as mentioned previously (Jahan et al., 2012).

IHCs, OHCs and IP cells were counted in the P7 control, *Atoh1-Cre; Atoh1*$^{f/kiNeurog1}$ and *Atoh1-Cre; Atoh1*$^{f/f}$ mice in 300 µm length in the comparable regions in the apex, middle and base of the cochlea after performing the immunohistochemistry of Myo7a and Tubulin. The quantification was performed in 6 independent cochleae from each different mouse genotype. For further details, see the supplementary Materials and Methods.

Statistical Analysis

The data obtained from the quantification of IHCs, OHCs and IP cells were analyzed using student's t-Test. The samples were referenced as statistically significant if $p<0.05$.

Auditory brainstem response (ABR) recording

Following sedation, ABR recording was performed in one month control and *Atoh1-Cre; Atoh1*$^{f/kiNeurog1}$ littermate mice. A loudspeaker was placed 10 cm away from the pinna of the test ear and computer-generated clicks were given in an open field environment in a soundproof chamber. Click responses were averaged and recorded signals were bandpass filtered (300 Hz–5 kHz) and 60Hz notch filter. The sound level was decreased in 10-dB steps from a 96-dB sound pressure level until there was no noticeable response. For further details, see the supplementary Materials and Methods.

Scanning electron microscopy (SEM)

SEM was performed as previously described (Jahan et al., 2012). Detailed description is in supplementary Materials and Methods.

Acknowledgements

We gratefully thank Dr. Fernando Giráldez for his constructive and valuable comments on our manuscript. We also thank the following people for providing plasmids for *in situ* hybridization: Qiufu Ma (*Neurog1*), Huda Y. Zoghbi *(Atoh1*), Mengqing Xiang (*Barhl1* and *Pou4f3*), Jacqueline E. Lee (*Neurod1*), Ulla Pirvola (*Fgf8*), Thomas Gridley (*Jag1*), Brigid L. M. Hogan (*Fgf10*), Doris K. Wu (*Bmp4*), Andy Groves (*Hes5*) and Guillermo Oliver (*Prox1*). We also wish to thank Central Microscopy Research Facility for SEM, Roy J. Carver Center for Imaging for using Leica TCS SP5 confocal microscopy, Roy J. Carver Center for Genomics for Roche 480 Light Cycler and Iowa Center for Molecular Auditory Neuroscience (P 30; ICMAN) for ABR facility at the University of Iowa.

Contributions: IJ, NP and BF conceived the work, NP and JK performed mouse breeding and genotyping, IJ collected and analyzed the data, IJ and BF wrote the paper. All the authors read and agreed on the manuscript.

References:

Ahmed, M., Wong, E.Y., Sun, J., Xu, J., Wang, F., Xu, P.X., 2012. Eya1-Six1 interaction is sufficient to induce hair cell fate in the cochlea by activating Atoh1 expression in cooperation with Sox2. Dev Cell 22, 377-390.

Benito-Gonzalez, A., Doetzlhofer, A., 2014. Hey1 and hey2 control the spatial and temporal pattern of mammalian auditory hair cell differentiation downstream of hedgehog signaling. The Journal of Neuroscience 34, 12865-12876.

Bermingham, N.A., Hassan, B.A., Price, S.D., Vollrath, M.A., Ben-Arie, N., Eatock, R.A., Bellen, H.J., Lysakowski, A., Zoghbi, H.Y., 1999. Math1: an essential gene for the generation of inner ear hair cells. Science 284, 1837-1841.

Brooker, R., Hozumi, K., Lewis, J., 2006. Notch ligands with contrasting functions: Jagged1 and Delta1 in the mouse inner ear. Development 133, 1277-1286.

Bustin, S.A., Benes, V., Garson, J.A., Hellemans, J., Huggett, J., Kubista, M., Mueller, R., Nolan, T., Pfaffl, M.W., Shipley, G.L., Vandesompele, J., Wittwer, C.T., 2009. The MIQE guidelines: minimum information for publication of quantitative real-time PCR experiments. Clin Chem 55, 611-622.

Cai, H., Richter, C.-P., Chadwick, R.S., 2003. Motion analysis in the hemicochlea. Biophysical journal 85, 1929-1937.

Cai, T., Jen, H.-I., Kang, H., Klisch, T.J., Zoghbi, H.Y., Groves, A.K., 2015. Characterization of the Transcriptome of Nascent Hair Cells and Identification of Direct Targets of the Atoh1 Transcription Factor. The Journal of Neuroscience 35, 5870-5883.

Cai, T., Seymour, M.L., Zhang, H., Pereira, F.A., Groves, A.K., 2013. Conditional deletion of Atoh1 reveals distinct critical periods for survival and function of hair cells in the organ of Corti. The Journal of Neuroscience 33, 10110-10122.

Chellappa, R., Li, S., Pauley, S., Jahan, I., Jin, K., Xiang, M., 2008. Barhl1 regulatory sequences required for cell-specific gene expression and autoregulation in the inner ear and central nervous system. Molecular and cellular biology 28, 1905-1914.

Chen, K.H., Boettiger, A.N., Moffitt, J.R., Wang, S., Zhuang, X., 2015. Spatially resolved, highly multiplexed RNA profiling in single cells. Science, aaa6090.

Chonko, K.T., Jahan, I., Stone, J., Wright, M.C., Fujiyama, T., Hoshino, M., Fritzsch, B., Maricich, S.M., 2013. Atoh1 directs hair cell differentiation and survival in the late embryonic mouse inner ear. Dev Biol 381, 401-410.

Doetzlhofer, A., Basch, M.L., Ohyama, T., Gessler, M., Groves, A.K., Segil, N., 2009. Hey2 regulation by FGF provides a Notch-independent mechanism for maintaining pillar cell fate in the organ of Corti. Dev Cell 16, 58-69.

Driver, E.C., Sillers, L., Coate, T.M., Rose, M.F., Kelley, M.W., 2013. The Atoh1-lineage gives rise to hair cells and supporting cells within the mammalian cochlea. Dev Biol 376, 86-98.

Du, X., Jensen, P., Goldowitz, D., Hamre, K.M., 2007. Wild-type cells rescue genotypically< i> Math1</i>-null hair cells in the inner ears of chimeric mice. Developmental biology 305, 430-438.

Fritzsch, B., Beisel, K.W., Hansen, L.A., 2006. The molecular basis of neurosensory cell formation in ear development: a blueprint for hair cell and sensory neuron regeneration? Bioessays 28, 1181-1193.

Fritzsch, B., Dillard, M., Lavado, A., Harvey, N.L., Jahan, I., 2010a. Canal cristae growth and fiber extension to the outer hair cells of the mouse ear require Prox1 activity. PLoS One 5, e9377.

Fritzsch, B., Eberl, D.F., Beisel, K.W., 2010b. The role of bHLH genes in ear development and evolution: revisiting a 10-year-old hypothesis. Cell Mol Life Sci 67, 3089-3099.

Fritzsch, B., Jahan, I., Pan, N., Elliott, K., 2014a. Evolving gene regulation networks into cellular networks guiding adaptive behavior: an outline how single cells could have evolved into a centralized neurosensory system. Cell $ Tissue Research 378, 1-19.

Fritzsch, B., Jahan, I., Pan, N., Elliott, K.L., 2015. Evolving gene regulatory networks into cellular networks guiding adaptive behavior: an outline how single cells could have evolved into a centralized neurosensory system. Cell and tissue research 359, 295-313.
Fritzsch, B., Matei, V.A., Nichols, D.H., Bermingham, N., Jones, K., Beisel, K.W., Wang, V.Y., 2005. Atoh1 null mice show directed afferent fiber growth to undifferentiated ear sensory epithelia followed by incomplete fiber retention. Dev Dyn 233, 570-583.
Fritzsch, B., Pan, N., Jahan, I., Elliott, K., 2014b. Inner ear development: Building a spiral ganglion and an organ of Corti out of unspecified ectoderm. Cell & Tissue Research 367, 1-18.
Groves, A.K., Fekete, D.M., 2012. Shaping sound in space: the regulation of inner ear patterning. Development 139, 245-257.
Guillemot, F., 2007. Spatial and temporal specification of neural fates by transcription factor codes. Development 134, 3771-3780.
Helms, A.W., Abney, A.L., Ben-Arie, N., Zoghbi, H.Y., Johnson, J.E., 2000. Autoregulation and multiple enhancers control Math1 expression in the developing nervous system. Development 127, 1185-1196.
Hertzano, R., Montcouquiol, M., Rashi-Elkeles, S., Elkon, R., Yücel, R., Frankel, W.N., Rechavi, G., Möröy, T., Friedman, T.B., Kelley, M.W., 2004. Transcription profiling of inner ears from Pou4f3ddl/ddl identifies Gfi1 as a target of the Pou4f3 deafness gene. Human molecular genetics 13, 2143-2153.
Hertzano, R., Shalit, E., Rzadzinska, A.K., Dror, A.A., Song, L., Ron, U., Tan, J.T., Shitrit, A.S., Fuchs, H., Hasson, T., 2008. A Myo6 mutation destroys coordination between the myosin heads, revealing new functions of myosin VI in the stereocilia of mammalian inner ear hair cells. PLoS genetics 4, e1000207.
Hudspeth, A., 2014. Integrating the active process of hair cells with cochlear function. Nature Reviews Neuroscience 15, 600-614.
Huh, S.H., Jones, J., Warchol, M.E., Ornitz, D.M., 2012. Differentiation of the Lateral Compartment of the Cochlea Requires a Temporally Restricted FGF20 Signal. PLoS Biol 10, e1001231.
Imayoshi, I., Kageyama, R., 2014. bHLH factors in self-renewal, multipotency, and fate choice of neural progenitor cells. Neuron 82, 9-23.
Jacobo, A., Hudspeth, A., 2014. Reaction–diffusion model of hair-bundle morphogenesis. Proceedings of the National Academy of Sciences, 201417420.
Jacques, B.E., Montcouquiol, M.E., Layman, E.M., Lewandoski, M., Kelley, M.W., 2007. Fgf8 induces pillar cell fate and regulates cellular patterning in the mammalian cochlea. Development 134, 3021-3029.
Jahan, I., Pan, N., Kersigo, J., Calisto, L.E., Morris, K.A., Kopecky, B., Duncan, J.S., Beisel, K.W., Fritzsch, B., 2012. Expression of Neurog1 instead of Atoh1 can partially rescue organ of Corti cell survival. PLoS One 7, e30853.
Jahan, I., Pan, N., Kersigo, J., Fritzsch, B., 2010. Neurod1 suppresses hair cell differentiation in ear ganglia and regulates hair cell subtype development in the cochlea. PLoS One 5, e11661.
Jahan, I., Pan, N., Kersigo, J., Fritzsch, B., 2013. Beyond generalized hair cells: molecular cues for hair cell types. Hear Res 297, 30-41.
Johnston, R.J., Jr., Desplan, C., 2014. Interchromosomal communication coordinates intrinsically stochastic expression between alleles. Science 343, 661-665.
Kelly, M.C., Chang, Q., Pan, A., Lin, X., Chen, P., 2012. Atoh1 directs the formation of sensory mosaics and induces cell proliferation in the postnatal mammalian cochlea in vivo. The Journal of neuroscience : the official journal of the Society for Neuroscience 32, 6699-6710.
Kersigo, J., Fritzsch, B., 2015a. Inner ear hair cells deteriorate in mice engineered to have no or diminished innervation. Frontiers in Aging Neuroscience 7.
Kersigo, J., Fritzsch, B., 2015b. Inner ear hair cells deteriorate in mice engineered to have no or diminished innervation. Frontiers in aging neuroscience, in press.

Kiernan, A.E., Xu, J., Gridley, T., 2006. The Notch ligand JAG1 is required for sensory progenitor development in the mammalian inner ear. PLoS Genet 2, e4.
Kitajiri, S.-i., Sakamoto, T., Belyantseva, I.A., Goodyear, R.J., Stepanyan, R., Fujiwara, I., Bird, J.E., Riazuddin, S., Riazuddin, S., Ahmed, Z.M., 2010. Actin-bundling protein TRIOBP forms resilient rootlets of hair cell stereocilia essential for hearing. Cell 141, 786-798.
Kobayashi, T., Kageyama, R., 2014. Expression dynamics and functions of hes factors in development and diseases. Current topics in developmental biology 110, 263-283.
Kuhn, S., Johnson, S.L., Furness, D.N., Chen, J., Ingham, N., Hilton, J.M., Steffes, G., Lewis, M.A., Zampini, V., Hackney, C.M., Masetto, S., Holley, M.C., Steel, K.P., Marcotti, W., 2011. miR-96 regulates the progression of differentiation in mammalian cochlear inner and outer hair cells. Proc Natl Acad Sci U S A 108, 2355-2360.
Lee, S., Danielian, P.S., Fritzsch, B., McMahon, A.P., 1997. Evidence that FGF8 signalling from the midbrain-hindbrain junction regulates growth and polarity in the developing midbrain. Development 124, 959-969.
Lewis, M.A., Quint, E., Glazier, A.M., Fuchs, H., De Angelis, M.H., Langford, C., van Dongen, S., Abreu-Goodger, C., Piipari, M., Redshaw, N., Dalmay, T., Moreno-Pelayo, M.A., Enright, A.J., Steel, K.P., 2009. An ENU-induced mutation of miR-96 associated with progressive hearing loss in mice. Nature genetics 41, 614-618.
Li, S., Price, S.M., Cahill, H., Ryugo, D.K., Shen, M.M., Xiang, M., 2002. Hearing loss caused by progressive degeneration of cochlear hair cells in mice deficient for the Barhl1 homeobox gene. Development 129, 3523-3532.
Ma, Q., Anderson, D.J., Fritzsch, B., 2000. Neurogenin 1 null mutant ears develop fewer, morphologically normal hair cells in smaller sensory epithelia devoid of innervation. J Assoc Res Otolaryngol 1, 129-143.
Mao, C.-A., Cho, J.-H., Wang, J., Gao, Z., Pan, P., Tsai, W.-W., Frishman, L.J., Klein, W.H., 2013. Reprogramming amacrine and photoreceptor progenitors into retinal ganglion cells by replacing Neurod1 with Atoh7. Development 140, 541-551.
Mao, C.A., Wang, S.W., Pan, P., Klein, W.H., 2008. Rewiring the retinal ganglion cell gene regulatory network: Neurod1 promotes retinal ganglion cell fate in the absence of Math5. Development 135, 3379-3388.
Masuda, M., Pak, K., Chavez, E., Ryan, A.F., 2012. TFE2 and GATA3 enhance induction of POU4F3 and myosin VIIa positive cells in nonsensory cochlear epithelium by ATOH1. Developmental biology 372, 68-80.
Matei, V., Pauley, S., Kaing, S., Rowitch, D., Beisel, K.W., Morris, K., Feng, F., Jones, K., Lee, J., Fritzsch, B., 2005. Smaller inner ear sensory epithelia in Neurog 1 null mice are related to earlier hair cell cycle exit. Dev Dyn 234, 633-650.
Mizutari, K., Fujioka, M., Hosoya, M., Bramhall, N., Okano, H.J., Okano, H., Edge, A.S., 2013. Notch inhibition induces cochlear hair cell regeneration and recovery of hearing after acoustic trauma. Neuron 77, 58-69.
Mogensen, M.M., Rzadzinska, A., Steel, K.P., 2007. The deaf mouse mutant whirler suggests a role for whirlin in actin filament dynamics and stereocilia development. Cell motility and the cytoskeleton 64, 496-508.
Mueller, K.L., Jacques, B.E., Kelley, M.W., 2002. Fibroblast growth factor signaling regulates pillar cell development in the organ of corti. The Journal of neuroscience : the official journal of the Society for Neuroscience 22, 9368-9377.
Müller, U., Barr-Gillespie, P.G., 2015. New treatment options for hearing loss. Nature Reviews Drug Discovery 14, 346-365.
Pan, N., Jahan, I., Kersigo, J., Duncan, J.S., Kopecky, B., Fritzsch, B., 2012a. A novel Atoh1 "self-terminating" mouse model reveals the necessity of proper Atoh1 level and duration for hair cell differentiation and viability. PLoS One 7, e30358.

Pan, N., Jahan, I., Kersigo, J., Kopecky, B., Santi, P., Johnson, S., Schmitz, H., Fritzsch, B., 2011. Conditional deletion of Atoh1 using Pax2-Cre results in viable mice without differentiated cochlear hair cells that have lost most of the organ of Corti. Hear Res 275, 66-80.
Pan, N., Jahan, I., Lee, J.E., Fritzsch, B., 2009. Defects in the cerebella of conditional Neurod1 null mice correlate with effective Tg(Atoh1-cre) recombination and granule cell requirements for Neurod1 for differentiation. Cell and tissue research 337, 407-428.
Pan, N., Kopecky, B., Jahan, I., Fritzsch, B., 2012b. Understanding the evolution and development of neurosensory transcription factors of the ear to enhance therapeutic translation. Cell Tissue Res.
Perrin, B.J., Sonnemann, K.J., Ervasti, J.M., 2010. β-actin and γ-actin are each dispensable for auditory hair cell development but required for stereocilia maintenance. PLoS genetics 6, e1001158.
Petrovic, J., Galvez, H., Neves, J., Abello, G., Giraldez, F., 2014. Differential regulation of Hes/Hey genes during inner ear development. Developmental neurobiology.
Pirvola, U., Spencer-Dene, B., Xing-Qun, L., Kettunen, P., Thesleff, I., Fritzsch, B., Dickson, C., Ylikoski, J., 2000. FGF/FGFR-2 (IIIb) signaling is essential for inner ear morphogenesis. The Journal of Neuroscience 20, 6125-6134.
Raft, S., Koundakjian, E.J., Quinones, H., Jayasena, C.S., Goodrich, L.V., Johnson, J.E., Segil, N., Groves, A.K., 2007. Cross-regulation of Ngn1 and Math1 coordinates the production of neurons and sensory hair cells during inner ear development. Development 134, 4405-4415.
Reiprich, S., Wegner, M., 2014. From CNS stem cells to neurons and glia: Sox for everyone. Cell and tissue research 363, 68-84.
Ronaghi, M., Nasr, M., Ealy, M., Durruthy-Durruthy, R., Waldhaus, J., Diaz, G.H., Joubert, L.M., Oshima, K., Heller, S., 2014. Inner ear hair cell-like cells from human embryonic stem cells. Stem cells and development 23, 1275-1284.
Rzadzinska, A.K., Nevalainen, E.M., Prosser, H.M., Lappalainen, P., Steel, K.P., 2009. MyosinVIIa interacts with Twinfilin-2 at the tips of mechanosensory stereocilia in the inner ear. PLoS One 4, e7097.
Schwander, M., Kachar, B., Müller, U., 2010. The cell biology of hearing. The Journal of cell biology 190, 9-20.
Sekerková, G., Richter, C.-P., Bartles, J.R., 2011. Roles of the espin actin-bundling proteins in the morphogenesis and stabilization of hair cell stereocilia revealed in CBA/CaJ congenic jerker mice. PLoS genetics 7, e1002032.
Self, T., Mahony, M., Fleming, J., Walsh, J., Brown, S., Steel, K.P., 1998. Shaker-1 mutations reveal roles for myosin VIIA in both development and function of cochlear hair cells. Development 125, 557-566.
Self, T., Sobe, T., Copeland, N.G., Jenkins, N.A., Avraham, K.B., Steel, K.P., 1999. Role of myosin VI in the differentiation of cochlear hair cells. Developmental biology 214, 331-341.
Sheykholeslami, K., Thimmappa, V., Nava, C., Bai, X., Yu, H., Zheng, T., Zhang, Z., Li, S.L., Liu, S., Zheng, Q.Y., 2013. A new mutation of the Atoh1 gene in mice with normal life span allows analysis of inner ear and cerebellar phenotype in aging. PLoS One 8, e79791.
Sienknecht, U.J., Köppl, C., Fritzsch, B., 2014. Evolution and Development of Hair Cell Polarity and Efferent Function in the Inner Ear. Brain, behavior and evolution 83, 150-161.
Slepecky, N.B., 1996. Structure of the mammalian cochlea, The cochlea. Springer, pp. 44-129.
Sprinzak, D., Lakhanpal, A., LeBon, L., Garcia-Ojalvo, J., Elowitz, M.B., 2011. Mutual inactivation of Notch receptors and ligands facilitates developmental patterning. PLoS computational biology 7, e1002069.
Tan, J., Clarke, M., Barrett, G., Millard, R., 2010. The p75 neurotrophin receptor protects primary auditory neurons against acoustic trauma in mice. Hearing research 268, 46-59.
Taylor, R., Bullen, A., Johnson, S.L., Grimm-Günter, E.-M., Rivero, F., Marcotti, W., Forge, A., Daudet, N., 2015. Absence of plastin 1 causes abnormal maintenance of hair cell stereocilia and a moderate form of hearing loss in mice. Human molecular genetics 24, 37-49.

Ueyama, T., Sakaguchi, H., Nakamura, T., Goto, A., Morioka, S., Shimizu, A., Nakao, K., Hishikawa, Y., Ninoyu, Y., Kassai, H., 2014. Maintenance of stereocilia and apical junctional complexes by Cdc42 in cochlear hair cells. Journal of cell science 127, 2040-2052.
von Bartheld, C.S., Patterson, S.L., Heuer, J.G., Wheeler, E.F., Bothwell, M., Rubel, E.W., 1991. Expression of nerve growth factor (NGF) receptors in the developing inner ear of chick and rat. Development 113, 455-470.
Wang, V.Y., Hassan, B.A., Bellen, H.J., Zoghbi, H.Y., 2002. Drosophila atonal fully rescues the phenotype of Math1 null mice: new functions evolve in new cellular contexts. Current biology : CB 12, 1611-1616.
Weston, M.D., Pierce, M.L., Jensen-Smith, H.C., Fritzsch, B., Rocha-Sanchez, S., Beisel, K.W., Soukup, G.A., 2011a. MicroRNA-183 family expression in hair cell development and requirement of microRNAs for hair cell maintenance and survival. Dev Dyn 240, 808-819.
Weston, M.D., Pierce, M.L., Jensen-Smith, H.C., Fritzsch, B., Rocha-Sanchez, S., Beisel, K.W., Soukup, G.A., 2011b. MicroRNA-183 family expression in hair cell development and requirement of microRNAs for hair cell maintenance and survival. Developmental dynamics 240, 808-819.
Xiang, M., Maklad, A., Pirvola, U., Fritzsch, B., 2003. Brn3c null mutant mice show long-term, incomplete retention of some afferent inner ear innervation. BMC Neuroscience 4, 2.
Yamamoto, S., Schulze, K.L., Bellen, H.J., 2014. Introduction to Notch Signaling, Notch Signaling. Springer, pp. 1-14.
Yang, S.M., Chen, W., Guo, W.W., Jia, S., Sun, J.H., Liu, H.Z., Young, W.Y., He, D.Z., 2012. Regeneration of stereocilia of hair cells by forced Atoh1 expression in the adult mammalian cochlea. PLoS One 7, e46355.
Zheng, J.L., Gao, W.Q., 2000. Overexpression of Math1 induces robust production of extra hair cells in postnatal rat inner ears. Nature neuroscience 3, 580-586.
Zine, A., Aubert, A., Qiu, J., Therianos, S., Guillemot, F., Kageyama, R., de Ribaupierre, F., 2001. Hes1 and Hes5 activities are required for the normal development of the hair cells in the mammalian inner ear. The Journal of neuroscience : the official journal of the Society for Neuroscience 21, 4712-4720.
Zine, A., de Ribaupierre, F., 2002. Notch/Notch ligands and Math1 expression patterns in the organ of Corti of wild-type and Hes1 and Hes5 mutant mice. Hear Res 170, 22-31.
Zine, A., Löwenheim, H., Fritzsch, B., 2014. Toward translating molecular ear development to generate hair cells from stem cells, Adult Stem Cells. Springer, pp. 111-161.

Figures

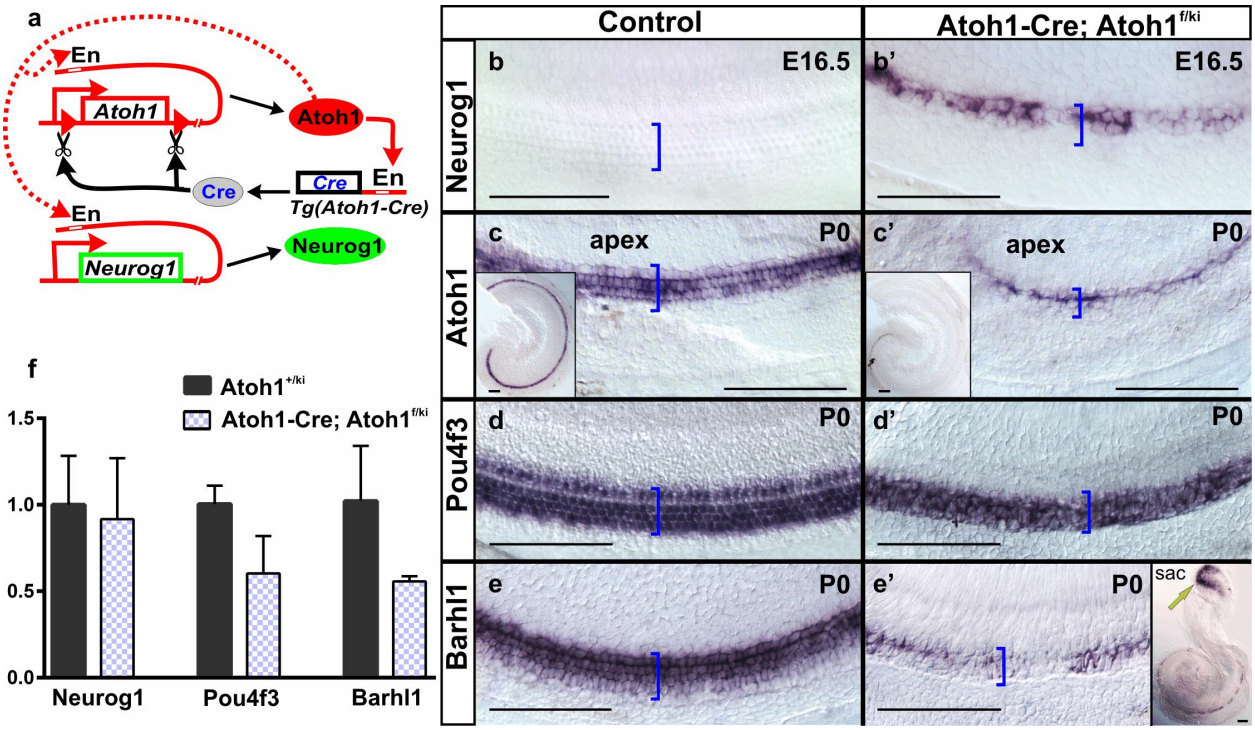

Figure 1. Our model combines *Atoh1-Cre*, a floxed *Atoh1* allele and an *Atoh1* allele replaced by *Neurog1* (a). *Atoh1-Cre* uses an Atoh1 enhancer (En) activated by Atoh1 protein to generate *Cre* to excise the floxed *Atoh1* allele. ISH shows misexpression of *Neurog1* in mutant HCs (b') and absence of *Neurog1* in control littermate (b). In contrast, *Atoh1* shows weak expression in one row of cells in the apical tip of the cochlea in *Atoh1-Cre; Atoh1*$^{f/kiNeurog1}$ mice (c' and insert) compared to broad expression in control littermate (c and insert). *Pou4f3* shows near identical expression in mutant and control littermates (d, d'). In contrast, *Barhl1* is reduced in the cochlea compared to vestibular epithelia (e', yellow arrow in insert in e') and control littermate (e). qPCR analysis reveals expression of *Neurog1*, *Pou4f3* and *Barhl1* in P7 cochlea (f). Relative expression of *Neurog1*, *Pou4f3* and *Barhl1* show reduction compared with *Atoh1*$^{+/kiNeurog1}$ cochlea (normalized to 1) (f). Bracket marks the OC. Bar indicates 100 µm.

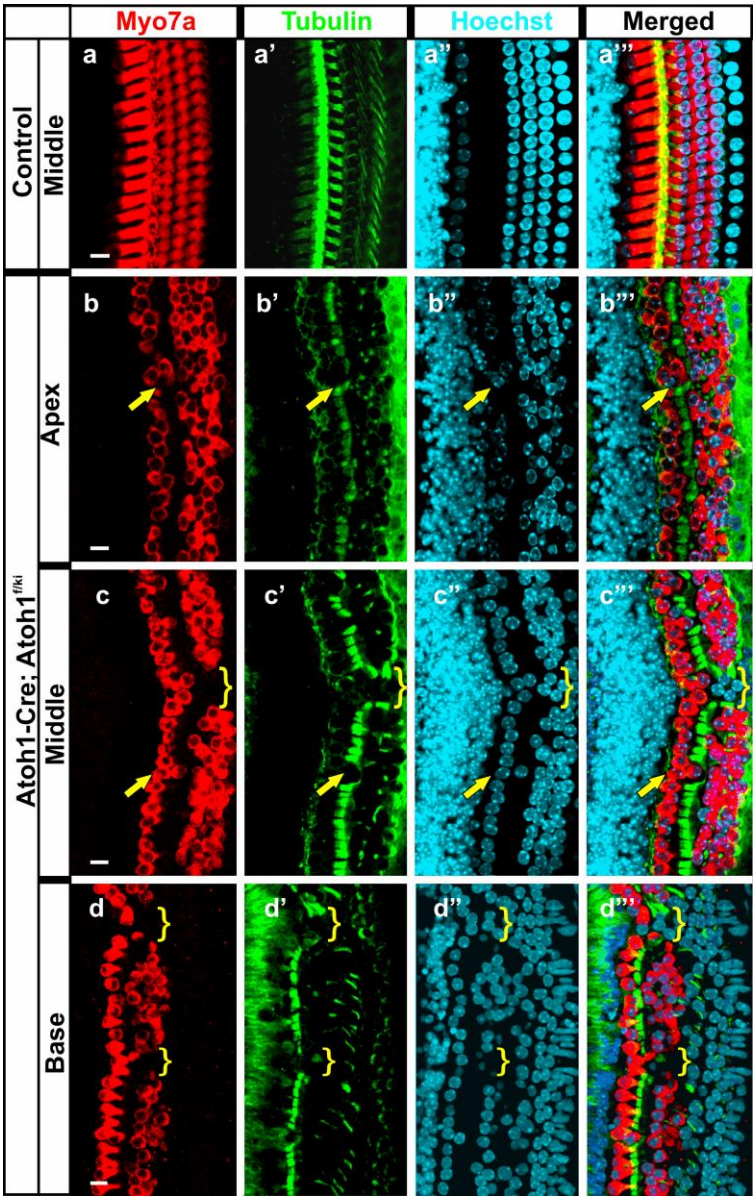

Figure 2. **Misexpression of *Neurog1* results in differentiation of HCs and SCs.** Myo7a (HCs) and Tubulin (SCs) immunohistochemistry in the P7 *Atoh1-Cre; Atoh1*$^{f/kiNeurog1}$ mice shows one row of IHCs and two-three rows of OHCs with near normal SCs (a-d'''). There is loss of third row of OHCs (d-d''') and gaps in OHCs (brackets in c-d''') toward the base of the cochlea. Some additional IHCs are associated with a loss of IP cells (yellow arrows in b-c'''). Bar indicates 10 μm.

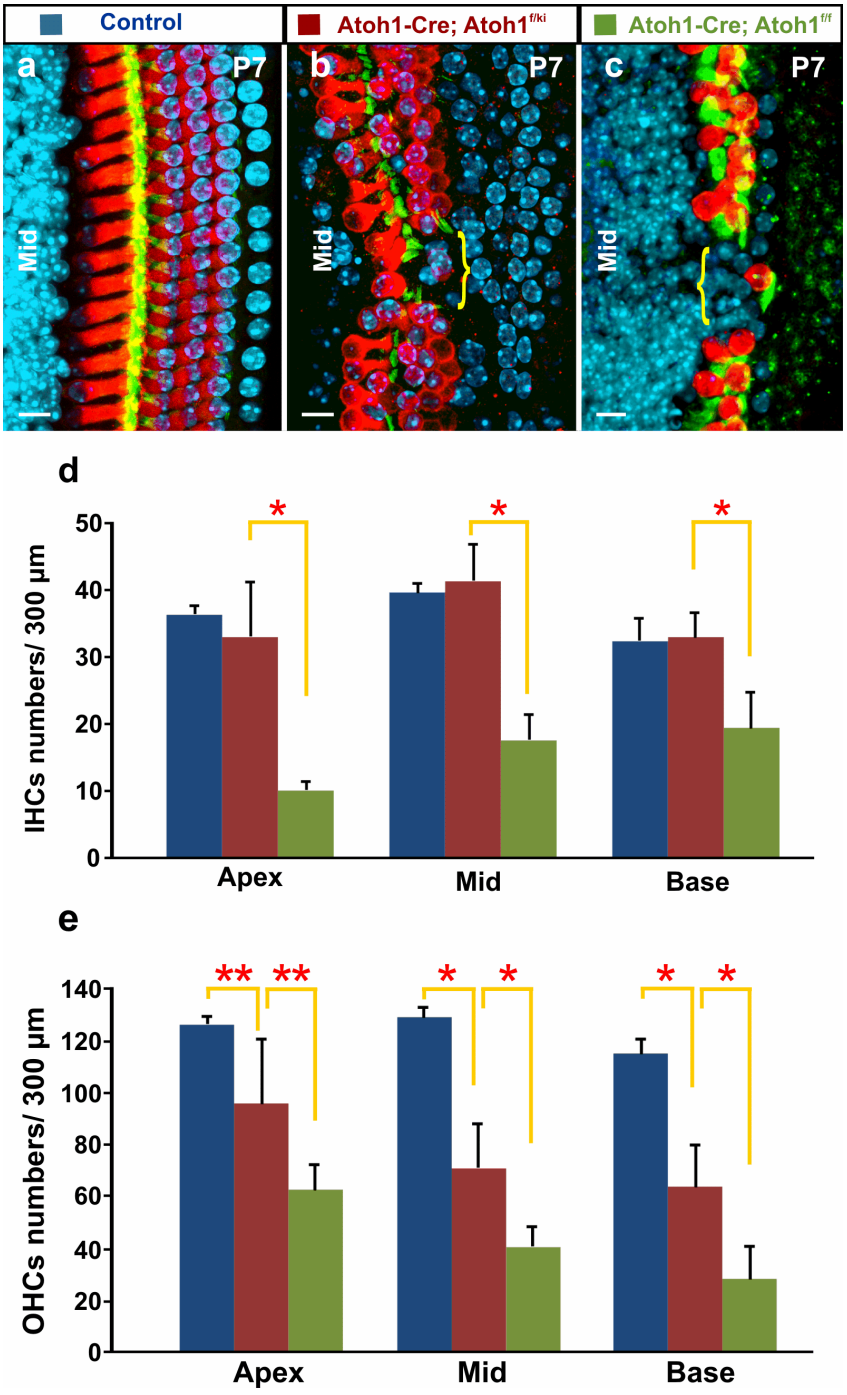

Figure 3. **Misexpression of *Neurog1* rescues IHCs formation.** Myo7a positive HCs in *Atoh1-Cre; Atoh1*$^{f/kiNeurog1}$ cochlea are compared with those in equivalent segments of *Atoh1-Cre; Atoh1*$^{f/f}$ and control littermates at P7 (a-c). *Atoh1-Cre; Atoh1*$^{f/kiNeurog1}$ cochlea has more HCs (b) in contrast to few patchy IHCs and one row of OHCs in the *Atoh1-Cre; Atoh1*$^{f/f}$ cochlea (c). Quantification of HCs reveals that the numbers of both IHCs and OHCs in the *Atoh1-Cre; Atoh1*$^{f/kiNeurog1}$ mice (red bar) are significantly higher than those in the *Atoh1-Cre;*

Atoh1$^{f/f}$ mice (green bar) but comparable to control littermates (blue bar) in all three areas (d). However, OHCs numbers are reduced in the *Atoh1-Cre; Atoh1*$^{f/kiNeurog1}$ mice compared to those in the control (blue bar; e), but are significantly above those in *Atoh1-Cre; Atoh1*$^{f/f}$ mice (green bar). Misexpression of *Neurog1* preferential rescues IHC formation. One or two Asterisks above SD bars indicates $p< 0.01$ or $p<0.05$, respectively. Bar indicates 10 µm.

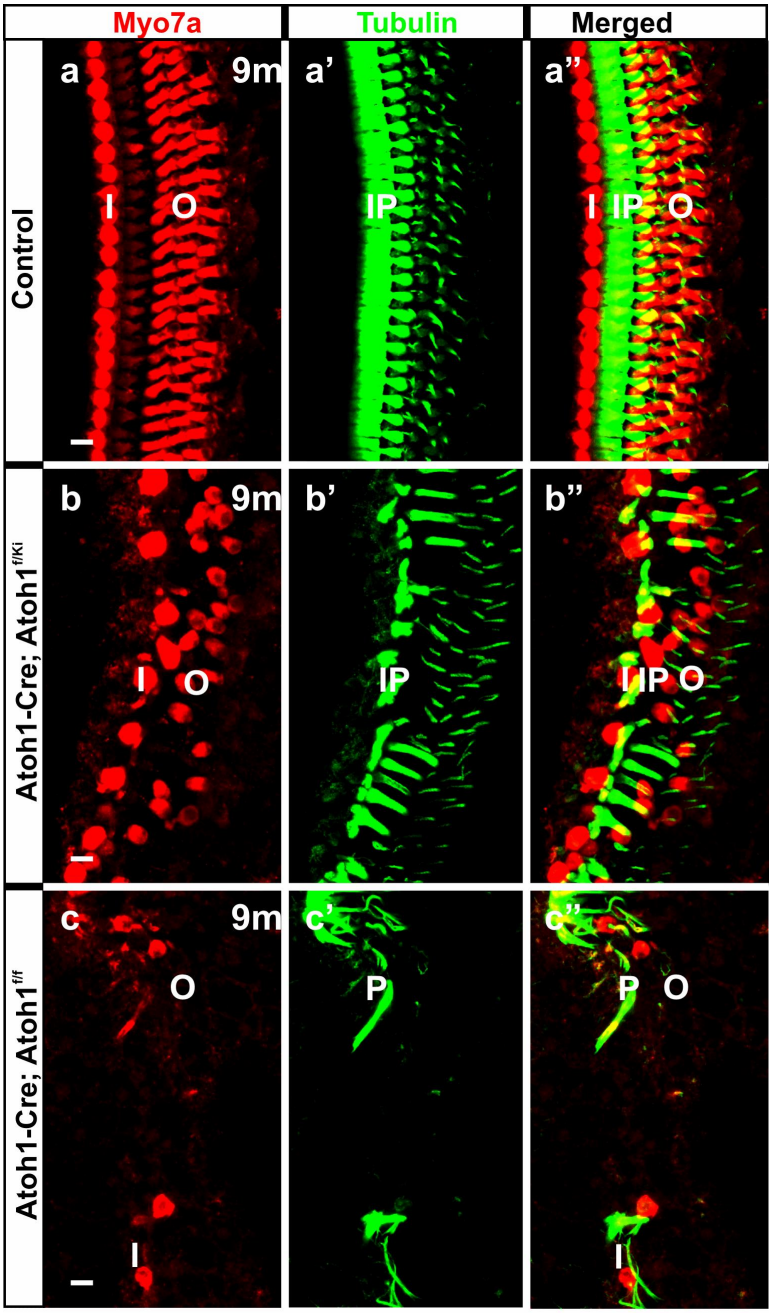

Figure 4. ***Neurog1*** **misexpression improves longevity of IHCs.** Immunohistochemistry of Myo7a and Tubulin show both IHCs and OHCs and many SCs survive until nine months in *Atoh1-Cre; Atoh1*$^{f/kiNeurog1}$ mice (b-b"). In contrast, some rare OHCs and SCs survive in the *Atoh1-Cre; Atoh1*$^{f/f}$ littermate (c-c"). Bar indicates 10 um.

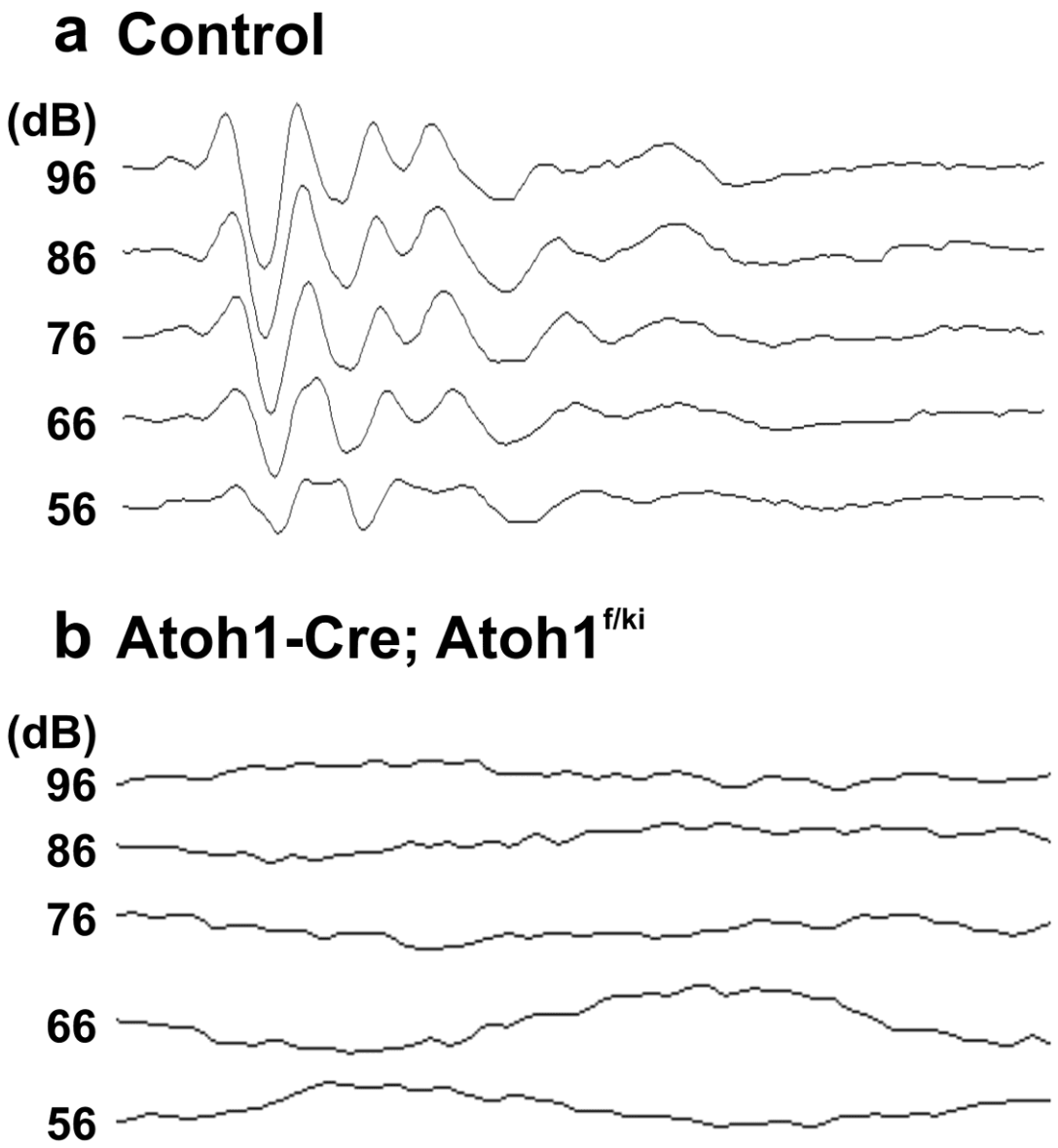

Figure 5. ***Atoh1-Cre; Atoh1$^{f/kiNeurog1}$*** **mice show no ABR response.** P30 *Atoh1-Cre; Atoh1$^{f/kiNeurog1}$* mice show no click response in ABR compared to the control (a-b) indicating severe deafness over the intensity range tested.

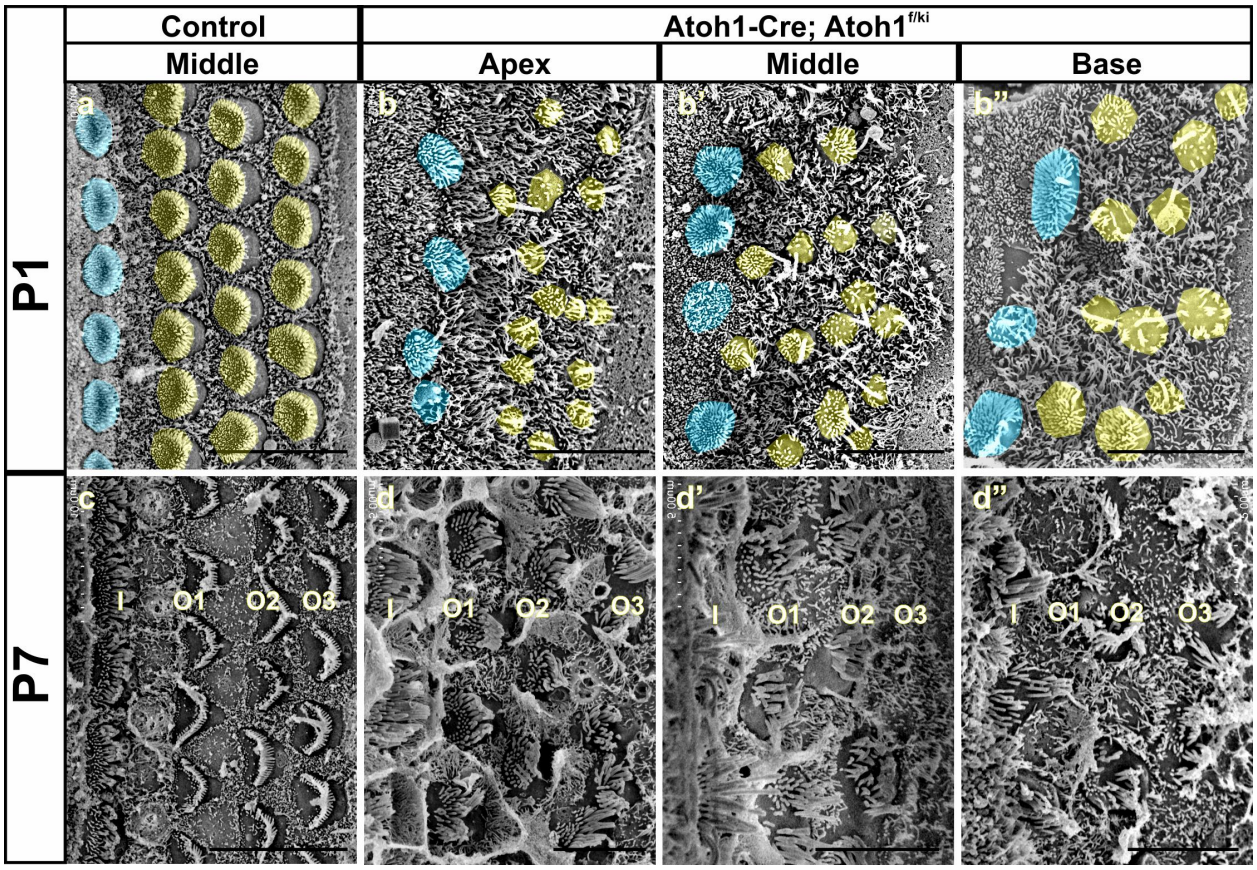

Figure 6. **Delayed onset of maturation of stereocilia bundle in *Atoh1-Cre; Atoh1*$^{f/kiNeurog1}$ mice.** SEM shows stereocilia bundles remain immature with central kinocilia at P1 in *Atoh1-Cre; Atoh1*$^{f/kiNeurog1}$ mice (b-b") and no stair-case pattern as in control littermates (a). This delay is most evident in the OHCs (b-b"). In P7 *Atoh1-Cre; Atoh1*$^{f/kiNeurog1}$ cochlea, the stereocilia bundles in the apical HCs form a near normal staircase pattern (d-d'), whereas the 3rd row of basal OHCs shows aberration (d"). A portion of HCs are color coded for better visibility, IHC as cyan and OHCs as yellow (a-b). Bar indicates 5 µm in all except 10 µm in c.

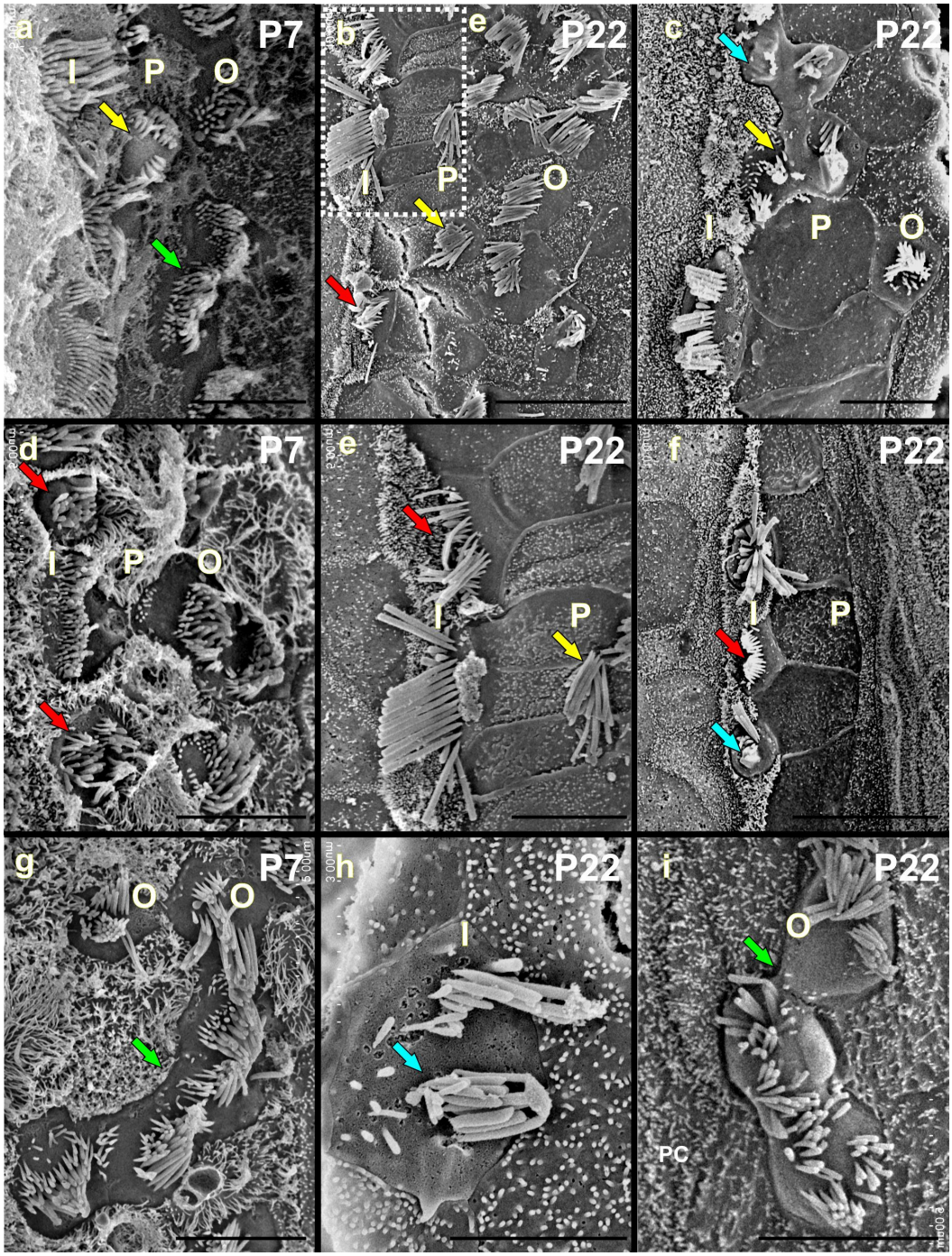

Figure 7. ***Neurog1*** **misexpression results in alteration in stereocilia bundle thickness, cell fate changes and disruption of cell-cell interactions.** Although *Neurog1* misexpression shows near normal HC formation (Figure 2-4), HC type and topology specific stereocilia bundle formation at P7 (a, d, g) and at P22 (b,c,e,f,h,i) is disorganized. Ectopic HCs form in the position of IP cells as revealed by formation of stereocilia bundles from their apical surfaces (yellow arrows in a-c, e). In addition, *Neurog1* misexpression results in

transdifferentiation of IHCs into OHCs demonstrated by the appearance of thin stereocilia of OHCs in the position of IHCs (red arrows in b, d, e, f). Some OHCs are in broad continuity with each other (green arrows in a, g, i) and some stereocilia bundles are fused or stunted in growth (cyan arrows in c, f, h). *Neurog1* misexpression results in irregular stereocilia formation in most HCs that gradually progress with age. Bar indicates 5 µm except b and f (10 µm) and i (3 µm).

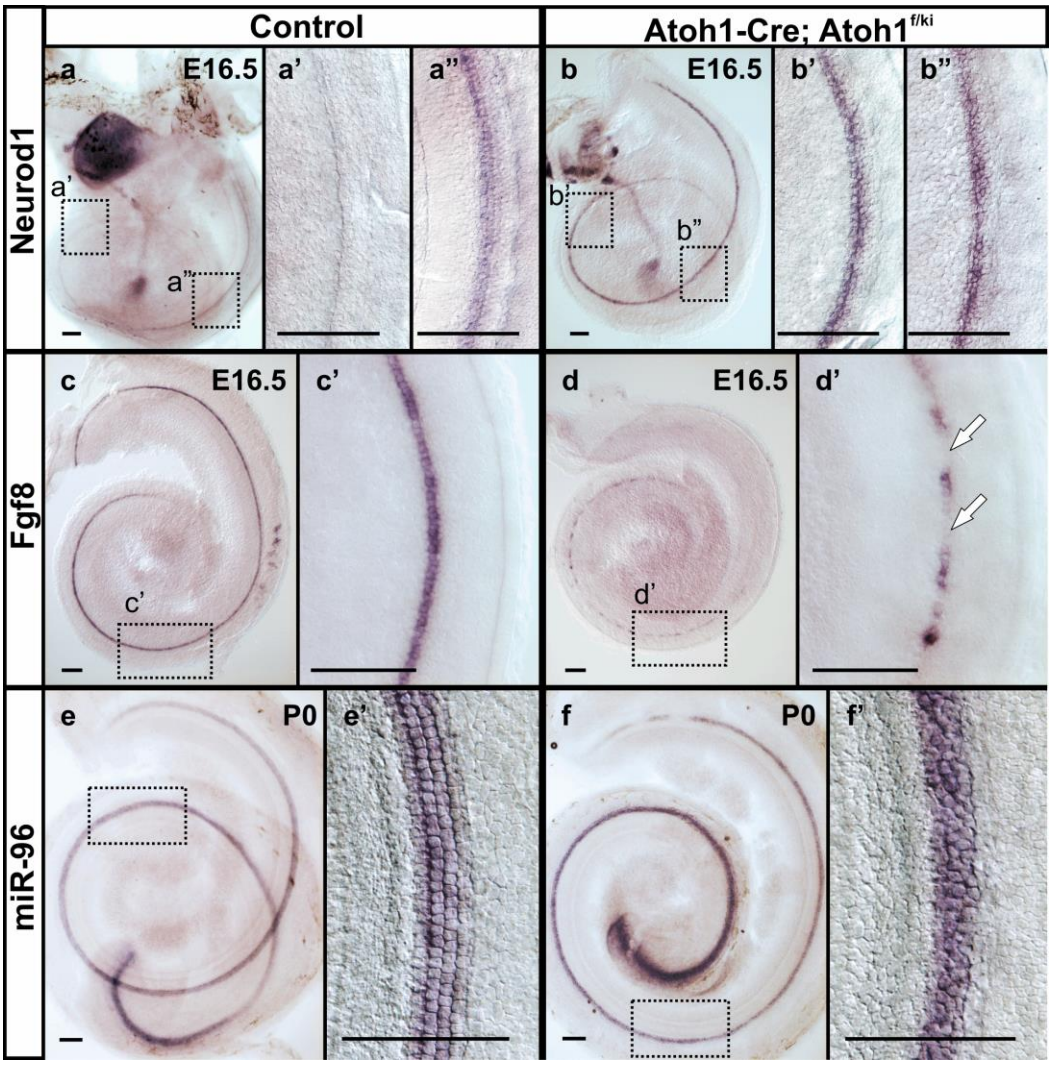

Figure 8. ***Neurog1*** **misexpression induces premature** ***Neurod1*** **upregulation and suppresses** ***Fgf8*** **but not** ***miR-96*** **expression.** ISH shows that expression of *Neurod1* expands both longitudinally and radially in the *Atoh1-Cre; Atoh1*$^{f/kiNeurog1}$ cochlea compared to the control littermate that is limited to IHCs (a-b"). *Fgf8* expression displays patchy downregulation in the E16.5 *Atoh1-Cre; Atoh1*$^{f/kiNeurog1}$ cochlea (c-d'). This suppression of *Fgf8* may in part be regulated by *Neurod1* overexpression in the *Atoh1-Cre; Atoh1*$^{f/kiNeurog1}$ mice (b-b"; d,d') as previously suggested (Jahan et al., 2010). *miR-96*, an essential microRNA for stereocilia differentiation, shows no expression changes in HCs (e-f). Bar indicates 100 µm.

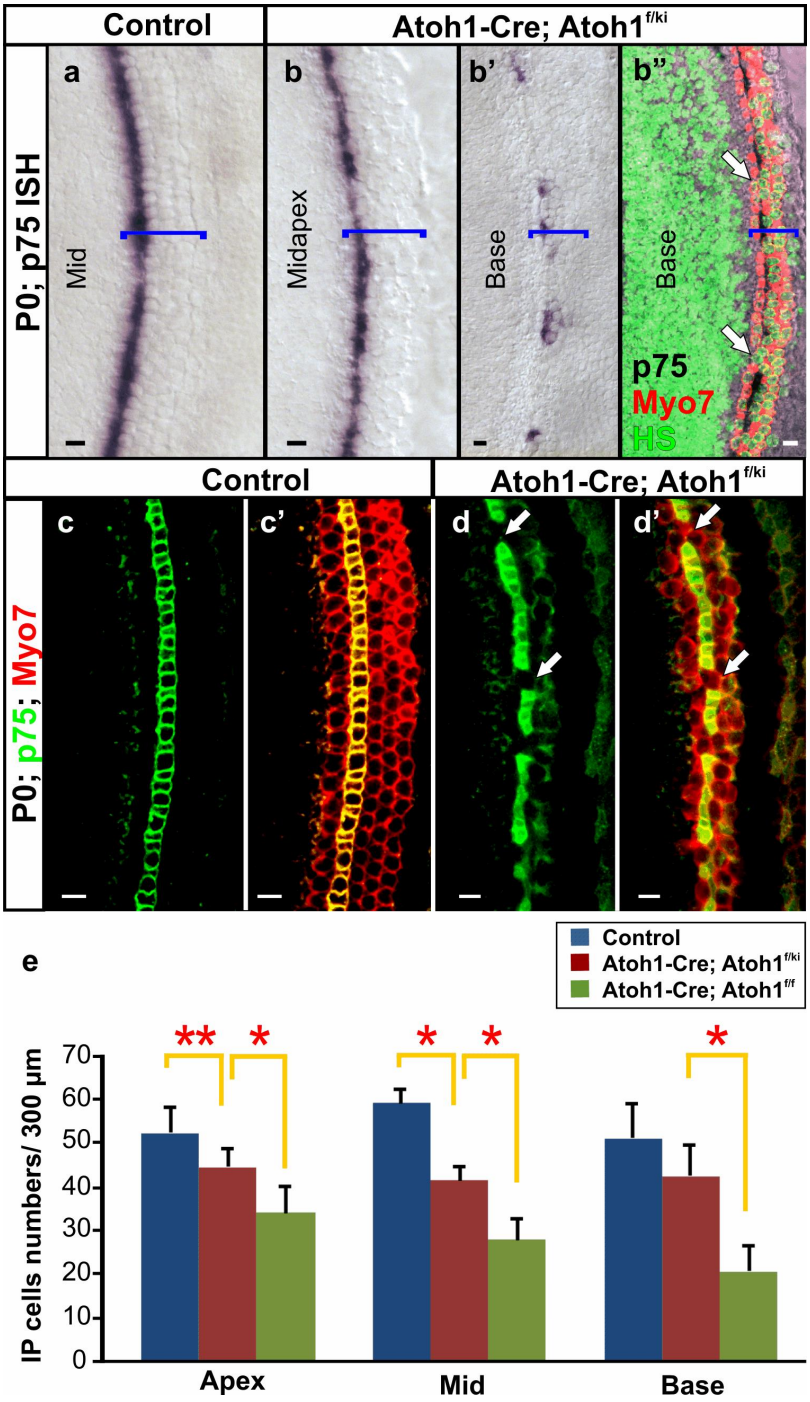

Figure 9. **Myo7a positive 'HCs' fill gaps of *p75* negative IP cells in *Atoh1-Cre; Atoh1$^{f/kiNeurog1}$* mice.** ISH of *p75* shows continuous expression in the IP cells in the apical half (mid) comparable to the control littermates but formation of gaps in the base (a,b-b"). Combining Myo7a immunohistochemistry with the *p75* ISH positive cochlea shows that some Myo7a positive 'HCs' form in the gaps of *p75* positive IP cells (white arrows in b") further confirmed by the double immunohistochemistry of p75 and Myo7a (white arrows in

d,d'). The quantification of the IP cells demonstrates decreased IP cells numbers in the *Atoh1-Cre; Atoh1*$^{f/kiNeurog1}$ mice (red bar) compared to control littermates (blue bar), but significantly increased compared to those in *Atoh1-Cre; Atoh1*$^{f/f}$ littermates (green bar). Bracket specifies the OC. Bar indicates 100 um. One Asterisk indicates $p< 0.01$ and two asterisks indicate $p<0.05$.

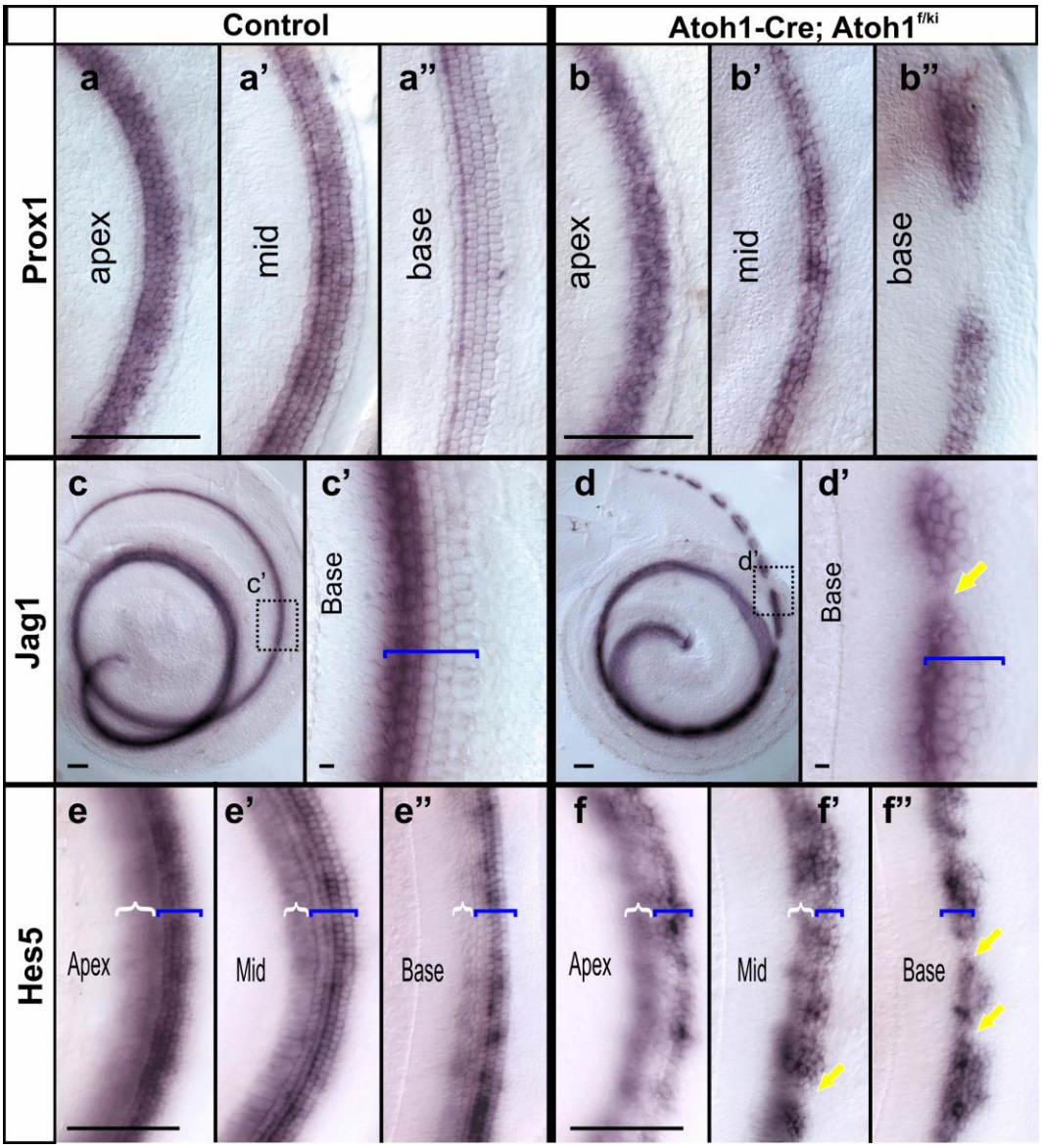

Figure 10. ***Neurog1* in HCs alters SC marker expression pattern.**

ISH reveals near normal expression of *Prox1* in SCs, except for some patchy loss in the base of the *Atoh1-Cre; Atoh1*$^{f/kiNeurog1}$ mice (a-b"). *Jag1* expression shows patchy loss (yellow arrows in d') in the *Atoh1-Cre; Atoh1*$^{f/kiNeurog1}$ mice. *Neurog1* misexpression results in differential loss of *Hes5* expression (yellow arrows in f', f"). '{'demarcates the expression in the GER and '[' in the OC. Bars indicate 100 µm in a-b", e-f" and 10 µm in c-d'.

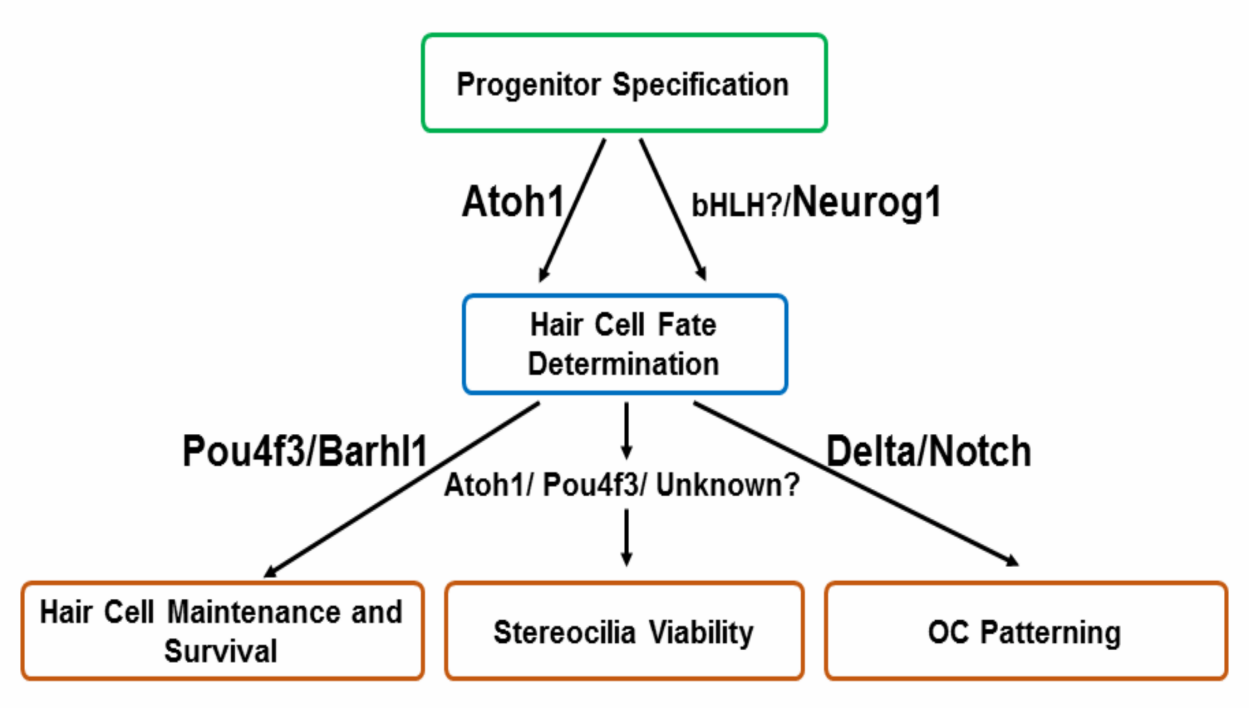

Figure 11. This summary flowchart indicates that *Atoh1* is essential for the HC fate determination, in part mediated by an unknown bHLH gene downstream of *Eya/Six1* (Ahmed et al., 2012). *Neurog1* may in part mimic this unknown bHLH gene to cooperate with *Atoh1* and to maintain expression of some target genes. However, *Neurog1* cannot fully regulate downstream HC genes associated with stereocilia maturation and OC patterning, leading to disorganization of the OC.

Supporting Information:

Supplementary Figures:

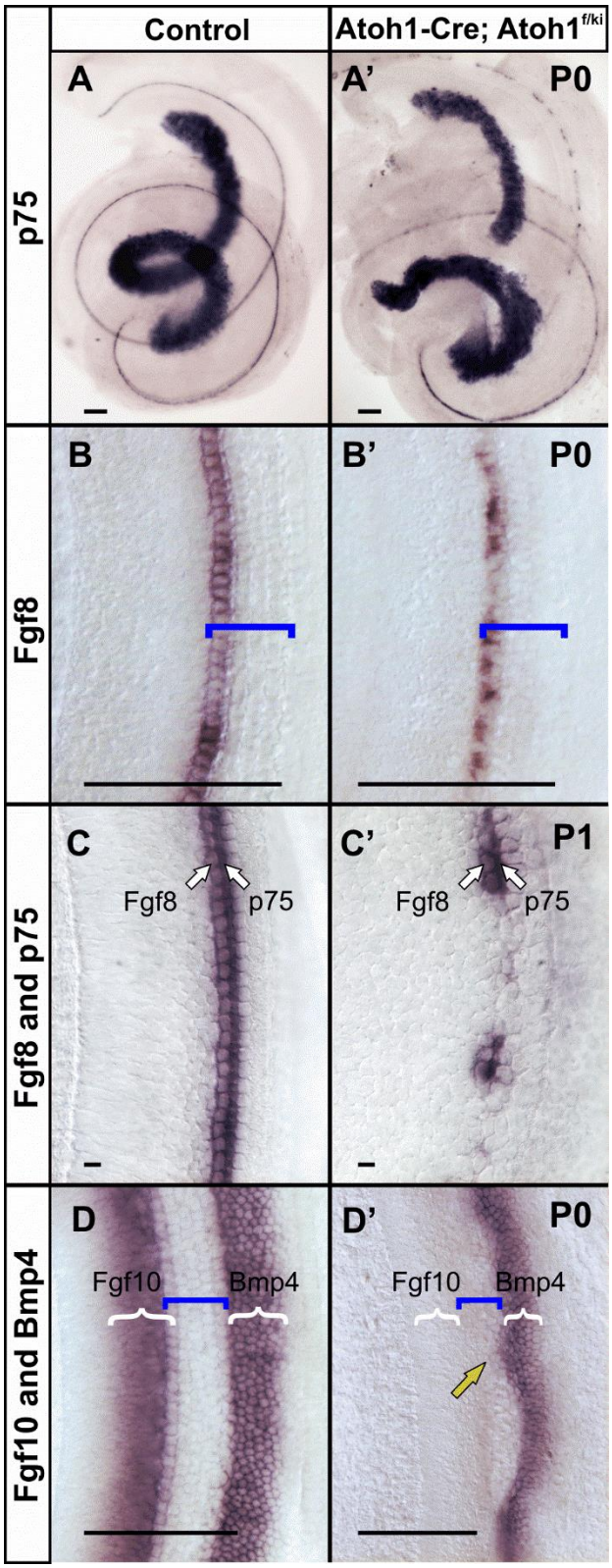

Figure S1. ***Fgf8* expression loss correlates with the *p75* expression loss and *Fgf10* and *Bmp4* are changed.** ISH of p75 reveals expression in the IP cells with a gradient from apex to base of the cochlea in the P0 *Atoh1-Cre; Atoh1*$^{f/kiNeurog1}$ mice (A, A'). *Fgf8* expression is also reduced in the IHC in the P0 *Atoh1-Cre; Atoh1*$^{f/kiNeurog1}$ mice (B, B'). Double ISH of *p75* and *Fgf8* in the P1 cochlea reveal that the loss of *Fgf8* expressing IHC correlates with the loss of *p75* positive IP cells (C,C'). Double ISH of *Fgf10* and *Bmp4* shows that *Fgf10* is nearly eliminated and *Bmp4* flanking the lateral/abneural boundary of the OC shows medial expansion in the *Atoh1-Cre; Atoh1*$^{f/kiNeurog1}$ mice (D, yellow arrow in D') like self-terminating mice (Pan et al., 2012a). Bar indicates 100 μm in all except 10 μm in C,C'.

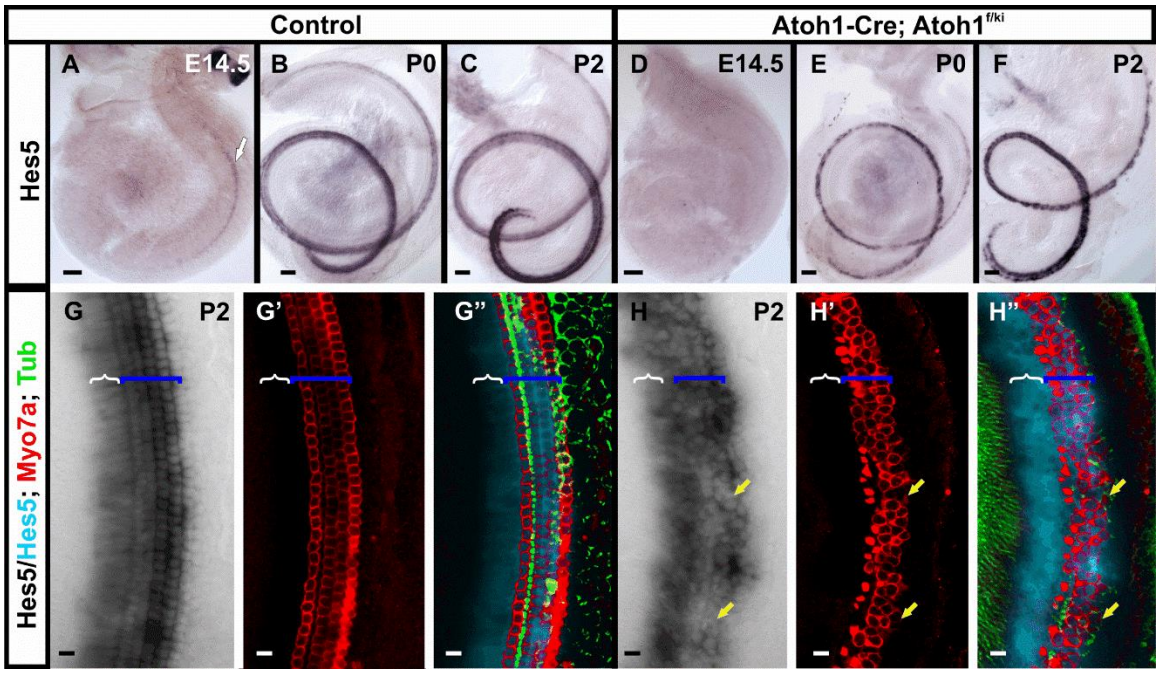

Figure S2. **Aberration of *Hes5* expression in the *Atoh1-Cre; Atoh1*$^{f/kiNeurog1}$ mice.** *Hes5* is upregulated in the mid-base of the control cochlea at E14.5 (A). *Hes5* is delayed in the littermate *Atoh1-Cre; Atoh1*$^{f/kiNeurog1}$ cochlea (D) that is upregulated later at P0 and P2 (E, F). *Hes5*, is dominantly expressed in the lateral SCs in the P2 control mice (G). In the *Atoh1-Cre; Atoh1*$^{f/kiNeurog1}$ mice, *Hes5* is differentially downregulated, particularly toward the base. Myo7a and Tubulin immunohistochemistry in the *Hes5* ISH reacted cochlea reveals that patchy downregulation of *Hes5* in *Atoh1-Cre; Atoh1*$^{f/kiNeurog1}$ mice is not associated with the quantitative changes of HCs (arrows in H-H") as reported in *Hes5* deletion mutants (Zine et al., 2001; Zine and de Ribaupierre, 2002). We use a false cyan color to show the ISH stain while combined with the immunohistochemistry. '{'demarcates the expression of *Hes5* in the GER and '[' in the OC. Bar indicates 100 µm in A-F and 10 µm in G-H".

Supplementary Tables:

Table S1. Total length measurement of the cochlea at P7. The total lengths of the cochleae at P7 display no substantial difference in both *Atoh1-Cre; Atoh1$^{f/kiNeurog1}$* and *Atoh1-Cre; Atoh1$^{f/f}$* mice compared to control littermates.

Total Length in µm	**Control**	***Atoh1-Cre; Atoh1$^{f/ki}$***	***Atoh1-Cre; Atoh1$^{f/f}$***
Mean (N=3)	6561±497	6523±187	6459±288

Table S2. The quantification of HCs and IP cells in the equivalent segments of the control, *Atoh1-Cre; Atoh1$^{f/kiNeurog1}$* and *Atoh1-Cre; Atoh1$^{f/f}$* cochlea at P7.

Mean of IHCs count (N=6)	**Control**	***Atoh1-Cre; Atoh1$^{f/ki}$***	***Atoh1-Cre; Atoh1$^{f/f}$***
Apex	37±1	33±8	10±1
Middle	40±1	42±5	18±4
Base	33±3	33±4	20±5
Mean of OHCs count	Control	*Atoh1-Cre; Atoh1$^{f/ki}$*	*Atoh1-Cre; Atoh1$^{f/f}$*
Apex	127±3	96±25	63±10
Middle	129±4	71±17	41±8
Base	115±6	64±16	28±13
Mean of IP cells count	Control	*Atoh1-Cre; Atoh1$^{f/ki}$*	*Atoh1-Cre; Atoh1$^{f/f}$*
Apex	53±6	45±4	34±6
Middle	59±3	42±3	28±5
Base	51±8	43±7	21±6

Table S3. Primer sequences used for the RT-qPCR are shown here.

Name	**Accession number**	**Primer Sequence**	**In silico Tm**	**% GC**	**Amplicon Length (bp)**
Neurog1	NM_010896.2	**Forward**: ggcctttgtaaggcaacatc **Reverse:** cagccagttccccatctatt	59/59	50/50	73
Pou4f3	NM_138945.2	**Forward**: ccccgtactgcaagaacc **Reverse:** catcaaagcttccaaatatattaccc	59/60	61/35	113
Barhl1	NM_019446.4	**Forward**: ggtaccagaaccgcagga **Reverse:** tggagcgccgagtaattg	59/60	61/56	88
Actb	NM_007393.3	**Forward**: ctaaggccaaccgtgaaaag **Reverse:** accagaggcatacagggaca	59/60	50/55	104

Supplementary Materials and Methods:

Genotyping

EconoTaq plus green 2X master mix (Lucigen, 30033) and a three primer sets were used for the genotyping of tail DNA. All resultant products were electrophoresed and visualized on a 2% agarose gel. The different primer sets were used to detect *Atoh1* floxed allele, *Atoh1*^{kiNeurog1} allele and *Cre*-specific primers to detect *Atoh1-Cre* transgene as described (Jahan et al., 2012; Pan et al., 2012a).

In situ hybridization

For *in situ* hybridization, the plasmids containing the cDNAs were used to generate the RNA probe by *in vitro* transcription. After being anesthetized with 2,2,2 tribromoethanol (Avertin), mice were perfused in 4% paraformaldehyde (PFA) and fixed overnight in 4% PFA. The ears were dissected in 0.4% PFA and dehydrated and rehydrated in graded methanol series and then digested briefly with 20 µg/ml of Proteinase K (Ambion, Austin, TX, USA) for 15-20 minutes. The samples were then hybridized overnight at 60°C to the riboprobe in hybridization solution. The samples were incubated overnight with an anti-digoxigenin antibody after washing off the unbound probe (Roche Diagnostics GmbH, Mannheim, Germany). After a series of washes, the samples were reacted with nitroblue phosphate/ 5-bromo, 4-chloro, 3-indolil phosphate (BM purple substrate, Roche Diagnostics, Germany) which is enzymatically converted to a purple colored product. The ears were mounted flat in glycerol and viewed in a Nikon Eclipse 800 microscope using differential interference contrast microscopy and images were captured with Metamorph software. The ears of the littermate of different genotype for the same gene expression were performed in the same reaction tubes to maintain the reaction accuracy.

Immunohistochemistry

For immunohistochemistry, decalcification was performed by incubating the postnatal ears in EDTA in 0.4% PFA before the microdissection. Then the ears were dehydrated in 100% ethanol and rehydrated in graded ethanol series and then washed in PBS and blocked with 2.5% normal goat serum in PBS containing 0.5% Triton-X-100 for 1 hour. Then the ears were incubated in

primary antibodies for Myo7a (Myosin 7a, Proteus Biosciences), tubulin (Sigma) and p75 (Sigma) in dilutions of 1:200, 1:800 and 1:1000 respectively for 24-48 hours at 4˚C. After several washes with PBS, corresponding secondary antibodies (1:500) (Alexa fluor molecular probe 647 or 532 or 488; Invitrogen) were added and incubated overnight at 4°C. Hoechst nuclear stain (Polysciences; 10mg/ml) was used at a dilution of 1:1000 at room temperature for 1 hour. The ears were washed with PBS and mounted in glycerol and images were taken with a Leica TCS SP5 confocal microscope.

Cell Counts

IHCs, OHCs and IP cells were counted in the comparable regions of P7 control, *Atoh1-Cre; Atoh1*$^{f/kiNeurog1}$ and *Atoh1-Cre; Atoh1*$^{f/f}$ cochleae after performing the immunohistochemistry of Myo7a and tubulin. Each cochlea was divided into 3 equal segments as apex, middle and base and the overview images (100x magnification) were taken to select the area for quantification. 10% distant from the apical tip was chosen for 'apex', 50% for 'Mid' and 90% for the 'base' quantification. Counting was performed on enlarged images at the 400x magnification in SP5 confocal microscope using the LIF software in the 300 µm stretch of apex, middle and base of the cochleae. LIF software allows computerized number markings after each count to facilitate accurate quantification. Tubulin positive IP cells were used to demarcate IHCs as medial to IP cells and OHCs as lateral to the IP cells.

Auditory brainstem response (ABR) recording

2,2,2 tribromoethanol (0.025 ml/g of body weight) was injected in one month old control and *Atoh1-Cre; Atoh1*$^{f/kiNeurog1}$ littermate mice and absence of ocular and pedal reflexes were assessed for surgical level of anesthesia. Needle electrodes were then inserted subcutaneously in the vertex, slightly posterior to the pinna and in the contralateral hind limb. A loudspeaker was placed 10 cm away from the pinna of the test ear and computer-generated clicks were given in an open field environment in a soundproof chamber. Click responses were averaged across 512 presentations using Tucker-Davis Technologies System hardware running BioSig® Software. Recorded signals were bandpass filtered (300 Hz–5 kHz) and 60Hz notch filter. The sound level was decreased in 10-dB steps from a 96-dB sound pressure level until there was no noticeable response.

Scanning electron microscopy (SEM)

The mice for SEM were perfused and fixed in 2.5% gluteraldehyde in 1% PFA after sedating with 2,2,2 tribromoethanol. Ears of postnatal mice were decalcified with EDTA. Following osmication in 2% osmium tetroxide in 0.1 M phosphate buffer (pH 7.4) for up to 1 hour, the ears were microdissected including removal of the Reissners membrane and the tectorial membrane. The samples were then washed several times with distilled water to remove ions, dehydrated in a graded ethanol series, critical point dried, mounted on stubs and coated with gold/palladium. Stubs were viewed with a Hitachi S-4800 Scanning Electron Microscope with 3MeV acceleration.